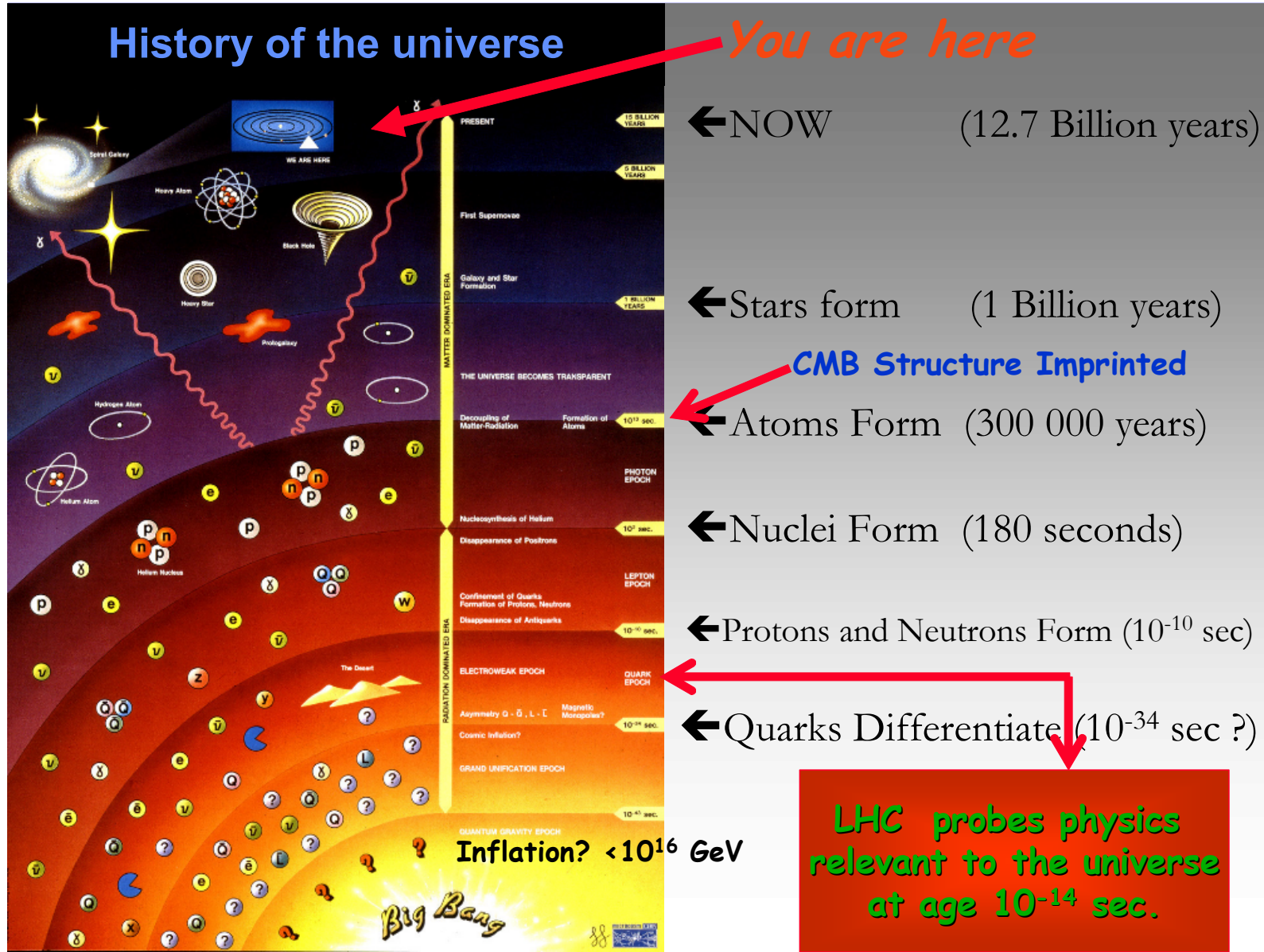


Next-Generation CMB Experiments and Technology

Helmuth Spieler

Lawrence Berkeley National Laboratory
Berkeley, CA 94720

1. Introduction
2. CMB Measurements
3. Examples of Existing CMB Arrays
4. Next-Generation Experiments
5. Cryogenic Detector Arrays
6. Summary
7. Outlook



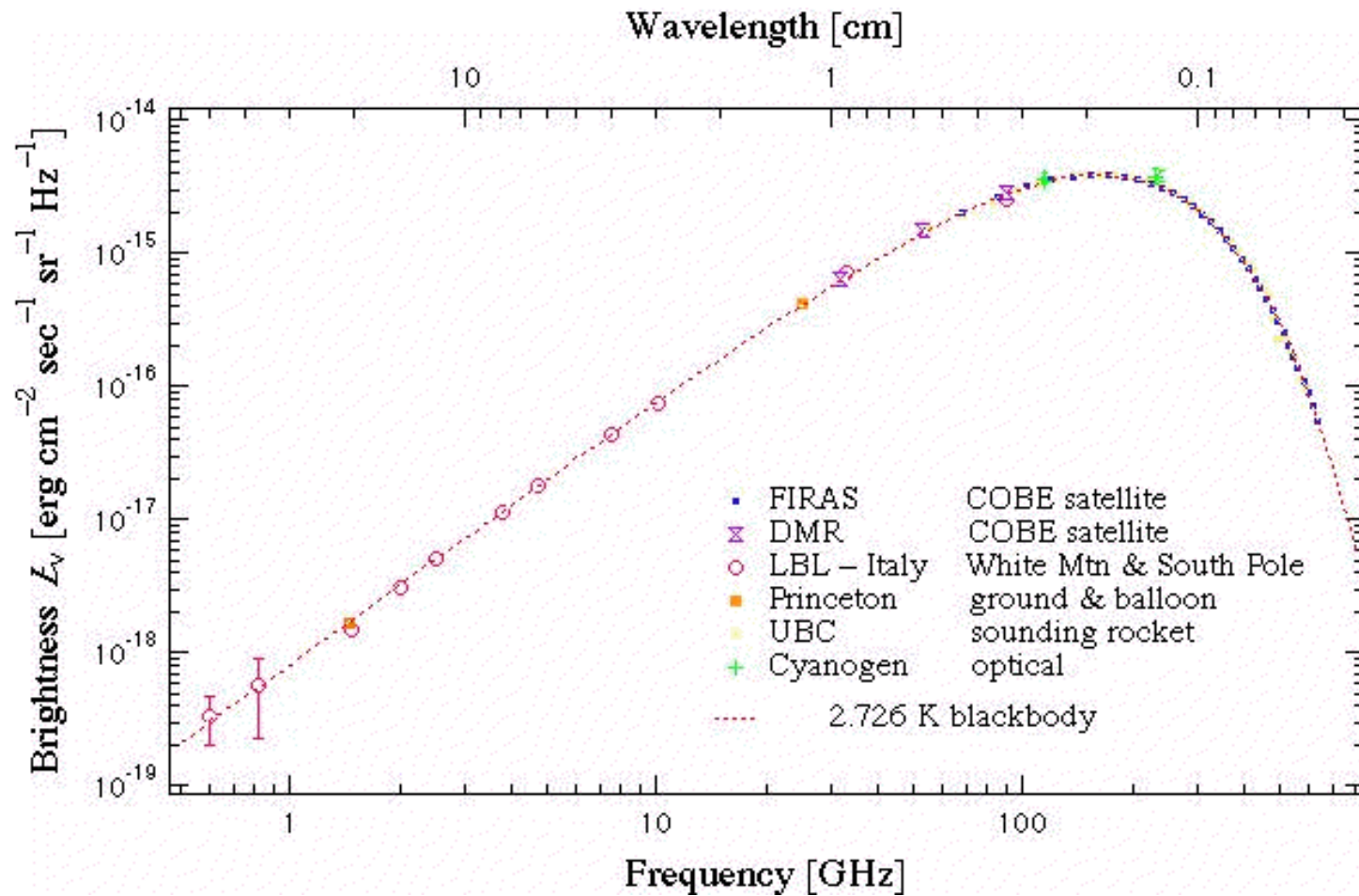
Inflation

- At $t \sim 10^{-38}$ s ABB, the universe undergoes a phase transition causing an explosive 10^{30} -fold exponential expansion
- Leaves its imprint as ***inflationary gravity waves***

Inflation predicts

- Cosmic Microwave Background radiation
- CMB is isotropic
- Exponential expansion locally flattens spatial curvature to high precision.
 - Universe is “flat” (Euclidian geometry)
- Density perturbations, which will eventually collapse under the pull of gravity to produce galaxies, stars,...

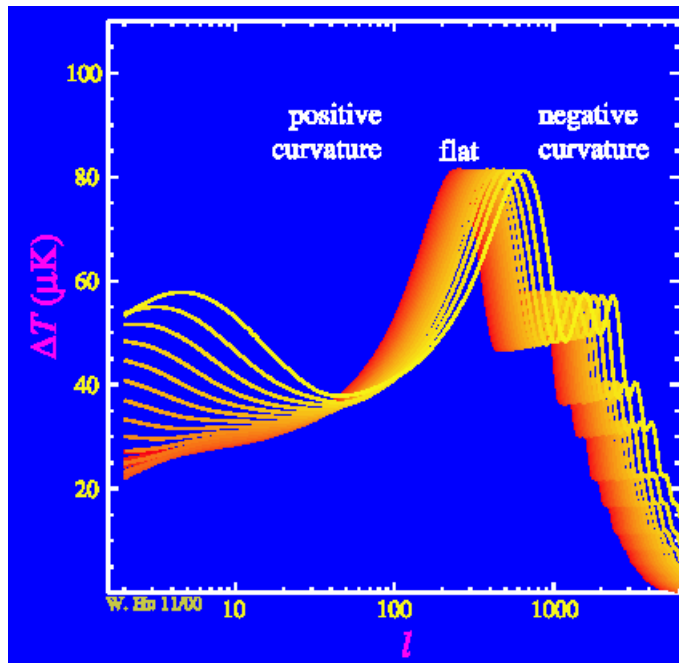
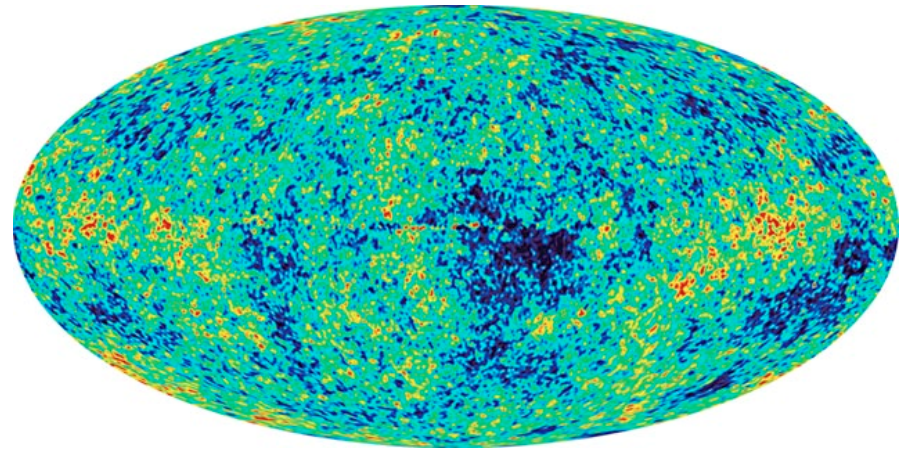
CMB has a near perfect black body spectrum ($T= 2.7\text{K}$)



Map Temperature of Sky:

Data from WMAP

Temperature anisotropy $\sim 10^{-5}$



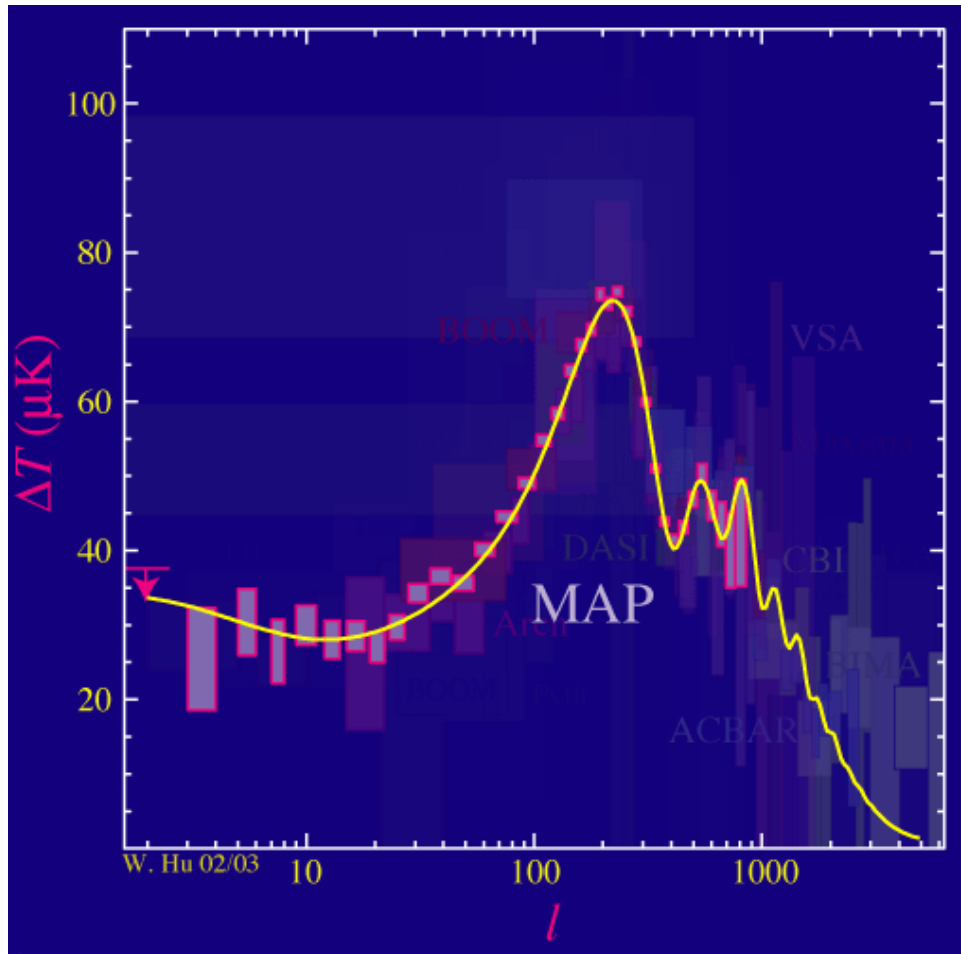
Multipole expansion of spatial distribution

Determine spectrum of angular scales

Dominant angular scale ~ 1 degree

Universe is flat

Multipole expansion of spatial distribution – determine angular scales

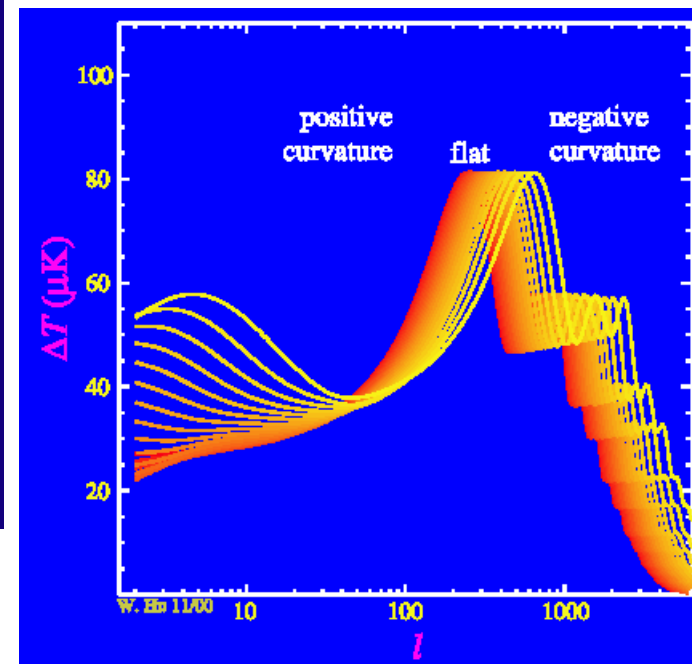


angular resolution $\Delta\Theta \approx 180/l$

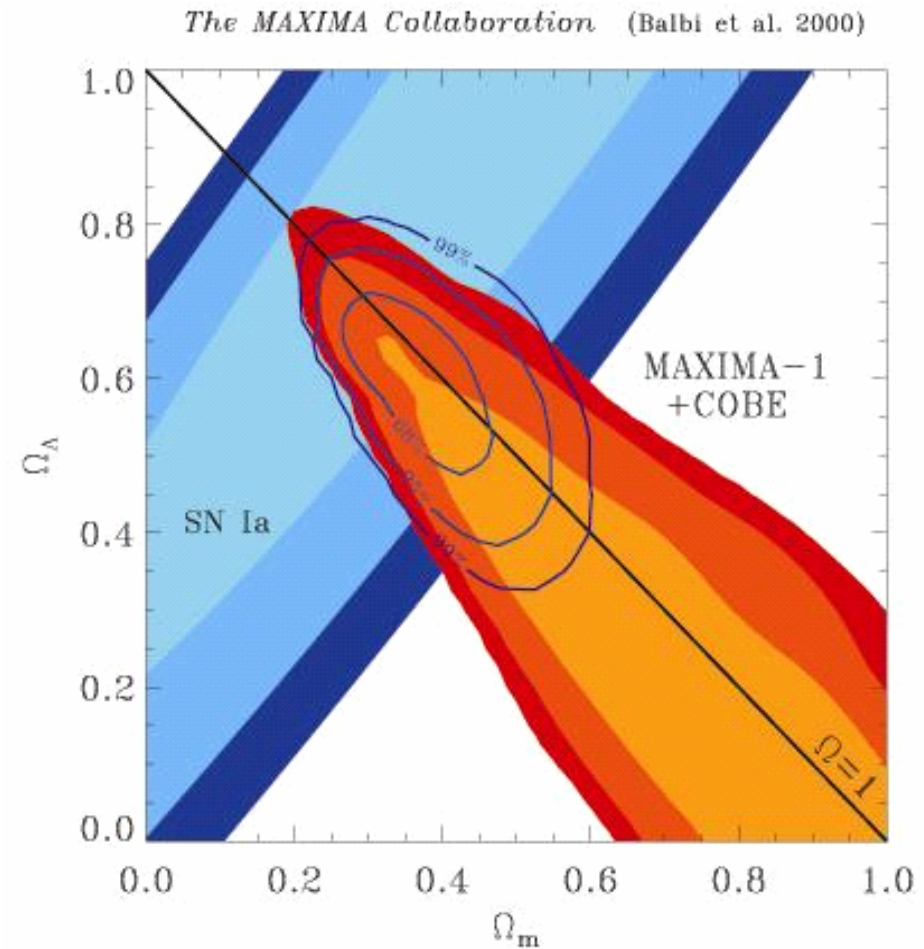
Angular structure depends on cosmological parameters

For example, geometry:

universe is flat



- CMB measurements provide constraints on fundamental cosmological parameters
- CMB spatial distribution largely unaffected since 300k yrs after Big Bang
- Supernova and CMB data *together* give best constraints on mass and energy density of the universe

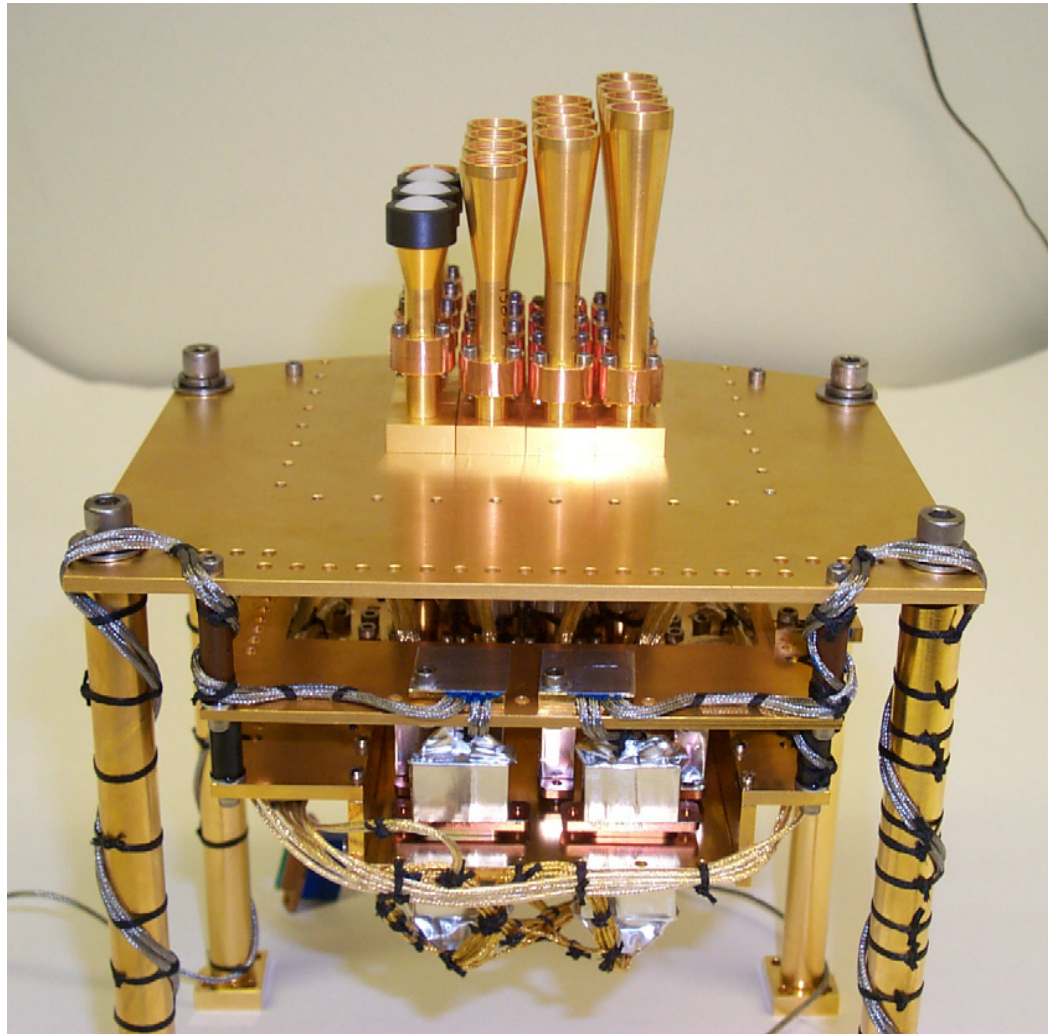


Measuring the CMB: 1. From the Ground

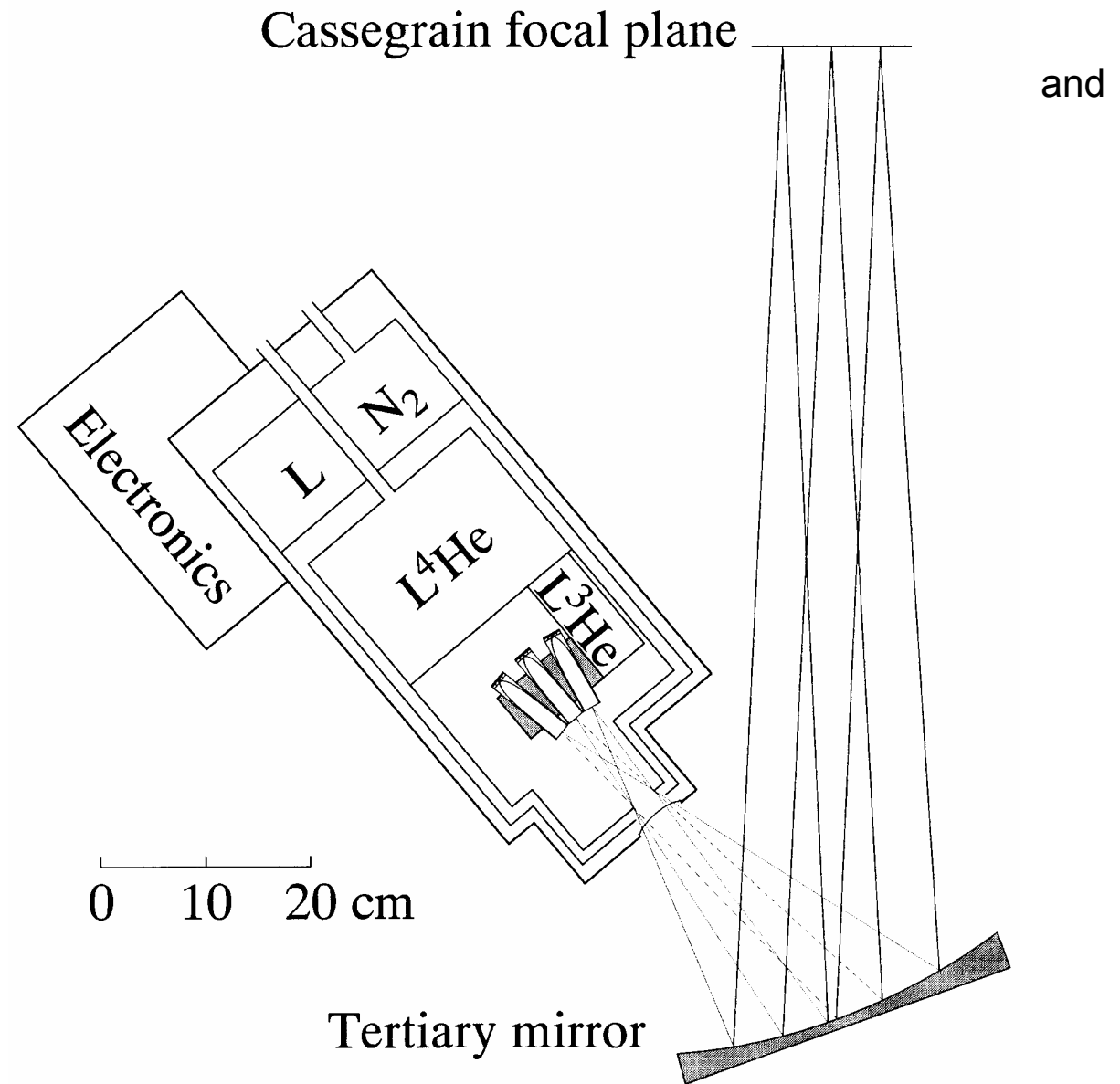


TODAY:
The VIPER Telescope at the South Pole

ACBAR focal plane array installed in Viper telescope
(Holzapfel et al.)

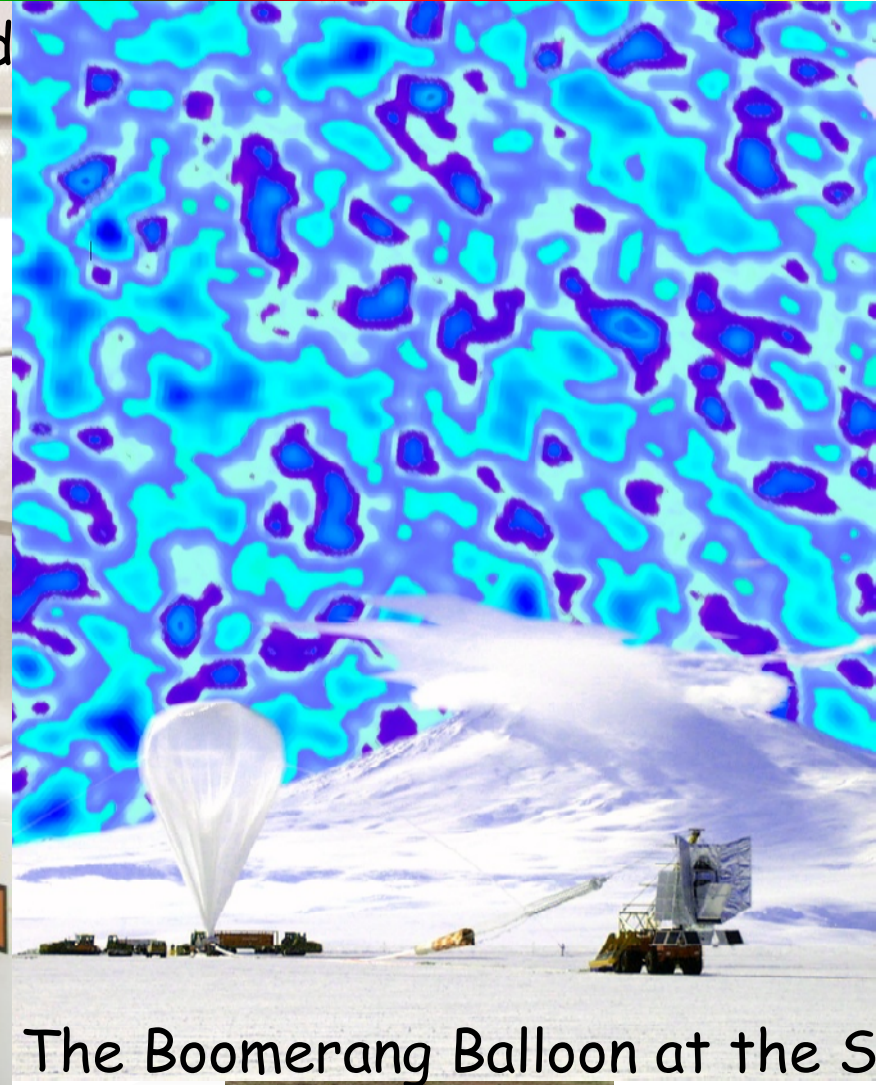
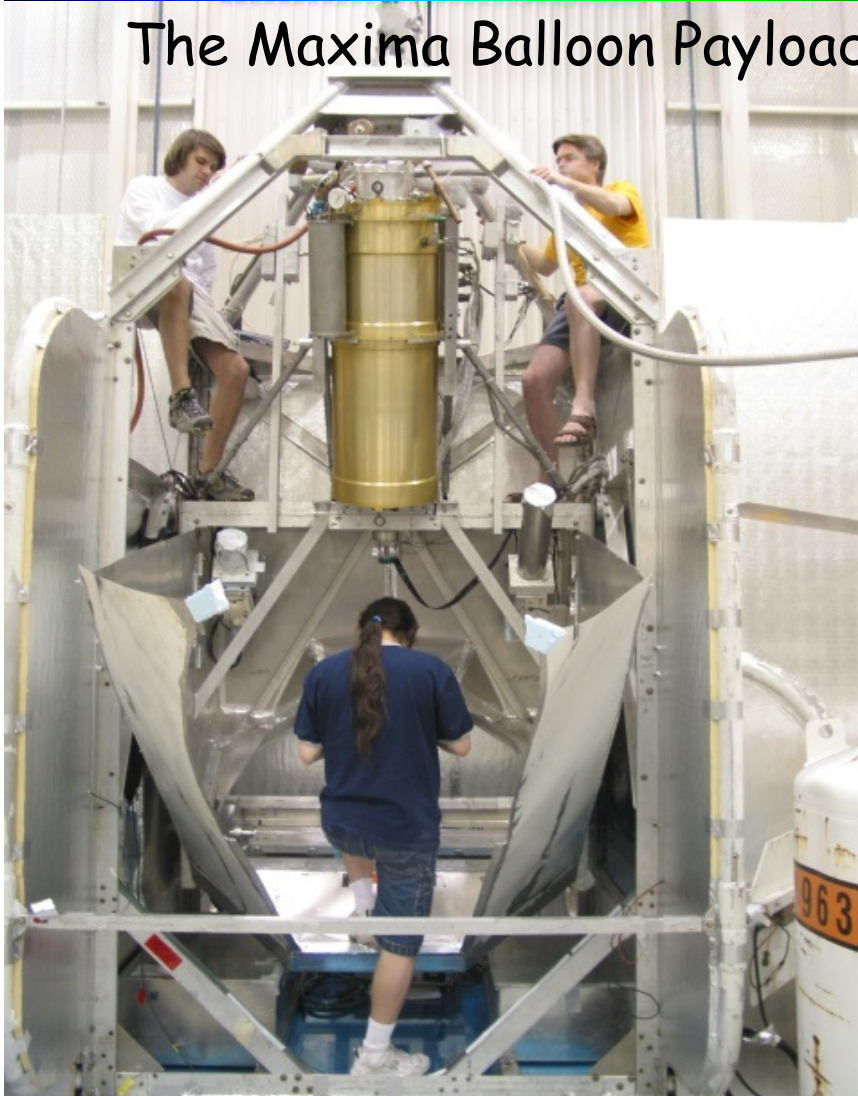


Layout of detector array
cryogenics



Measuring the CMB: 2. From Balloons

The Maxima Balloon Payload



The Boomerang Balloon at the S

Matt Dobbs <MADobbs@lbl.gov>

CMB Cosmology

QuarkNet July 25, 2003 41

*Next-Generation CMB Experiments and Technology
2003 ICFA Instrumentation School, Itacuruçá, Brazil*

*Helmuth Spieler
LBNL*

Measuring the CMB from Balloons

Maxima (P. Richards et al.)

Balloon-based experiment (launched in Texas)

Measure angular distribution of temperature variations

Gondola prior to launch

Measurements at ~40 km altitude



Detector array in focal plane

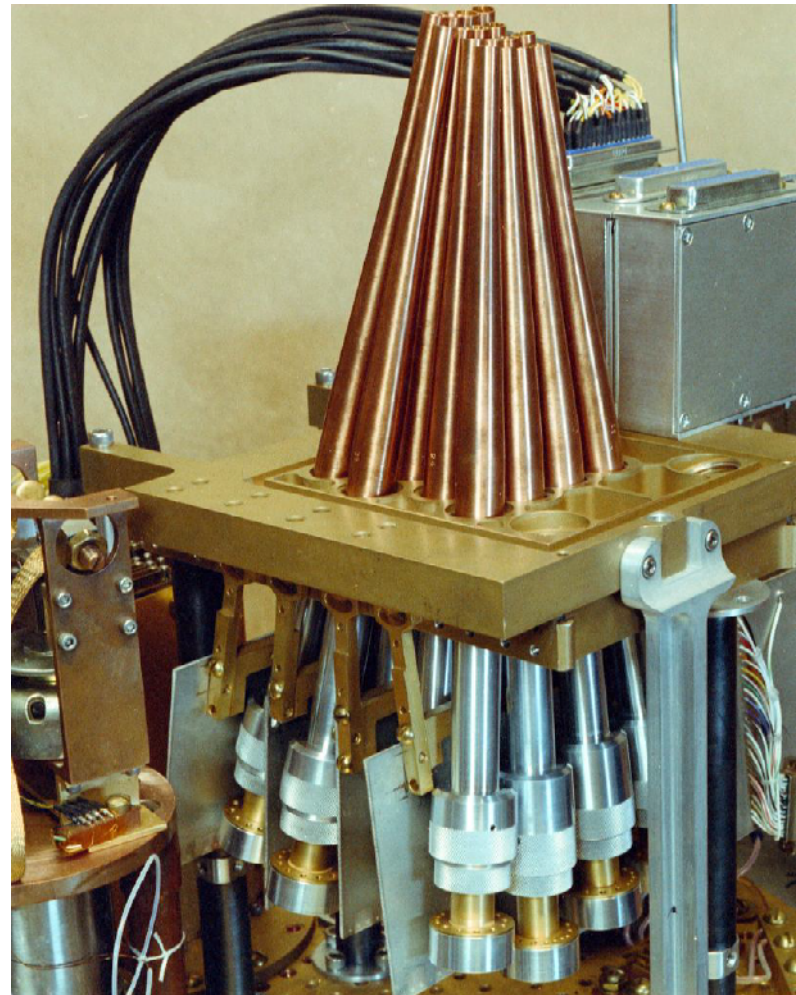
Bolometers absorb radiation directly and translate temperature rise into electrical signal.

Array of 16 horn antennas coupled to individual bolometers at 100 mK.

Angular resolution: 10' FWHM

Frequency bands: 150, 240 and 410 GHz
(~30 – 60 GHz BW)

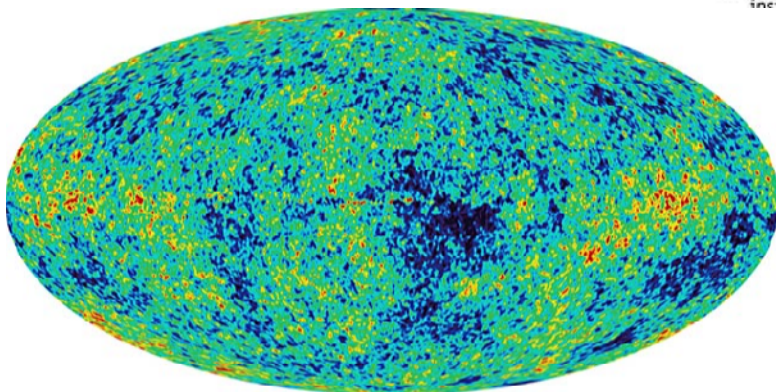
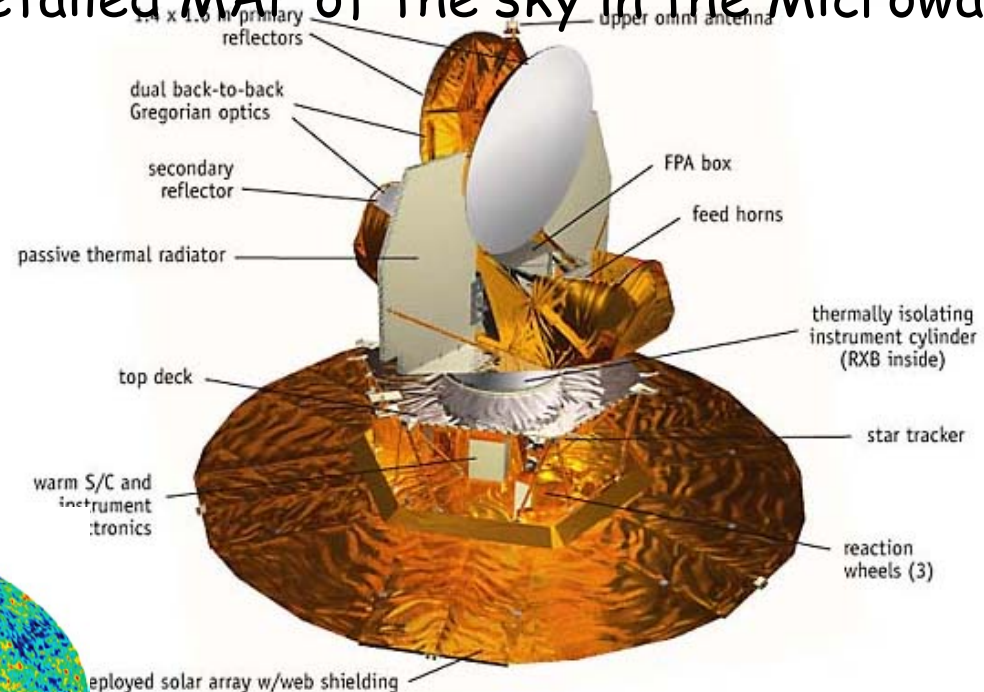
Sensitivity: $\sim 100 \text{ mK}/\sqrt{\text{Hz}}$



Measuring the CMB: 3. with Satellites



The Wilkinson Microwave Anisotropy Probe was launched in June 2002, producing the detailed MAP of the sky in the Microwave



A further advantage of satellites
full sky coverage.

Matt Dobbs <MADobbs@lbl.gov> CMB Cosmology QuarkNet July 25, 2003 42

Some Next Generation Experiments

| | |
|----------------------|-------------------------------------|
| APEX-SZ | UCB, LBNL, MPIfR |
| South Pole Telescope | Univ. Chicago, UCB, LBNL, CWRU, CfA |
| PolarBear | UCB, LBNL |

Berkeley Group

John Clarke (LBNL,UCB)
 William Holzapfel (UCB)
 Adrian Lee (LBNL,UCB)
 Paul Richards (UCB)
 Helmuth Spieler (LBNL)
 Martin White (LBNL,UCB)

John Joseph (Eng. Div. LBNL)
 Chinh Vu (Eng. Div. LBNL)

Sherry Cho (UCB)
 Matt Dobbs (LBNL)
 Nils Halverson (UCB)
 Huan Tran (UCB)

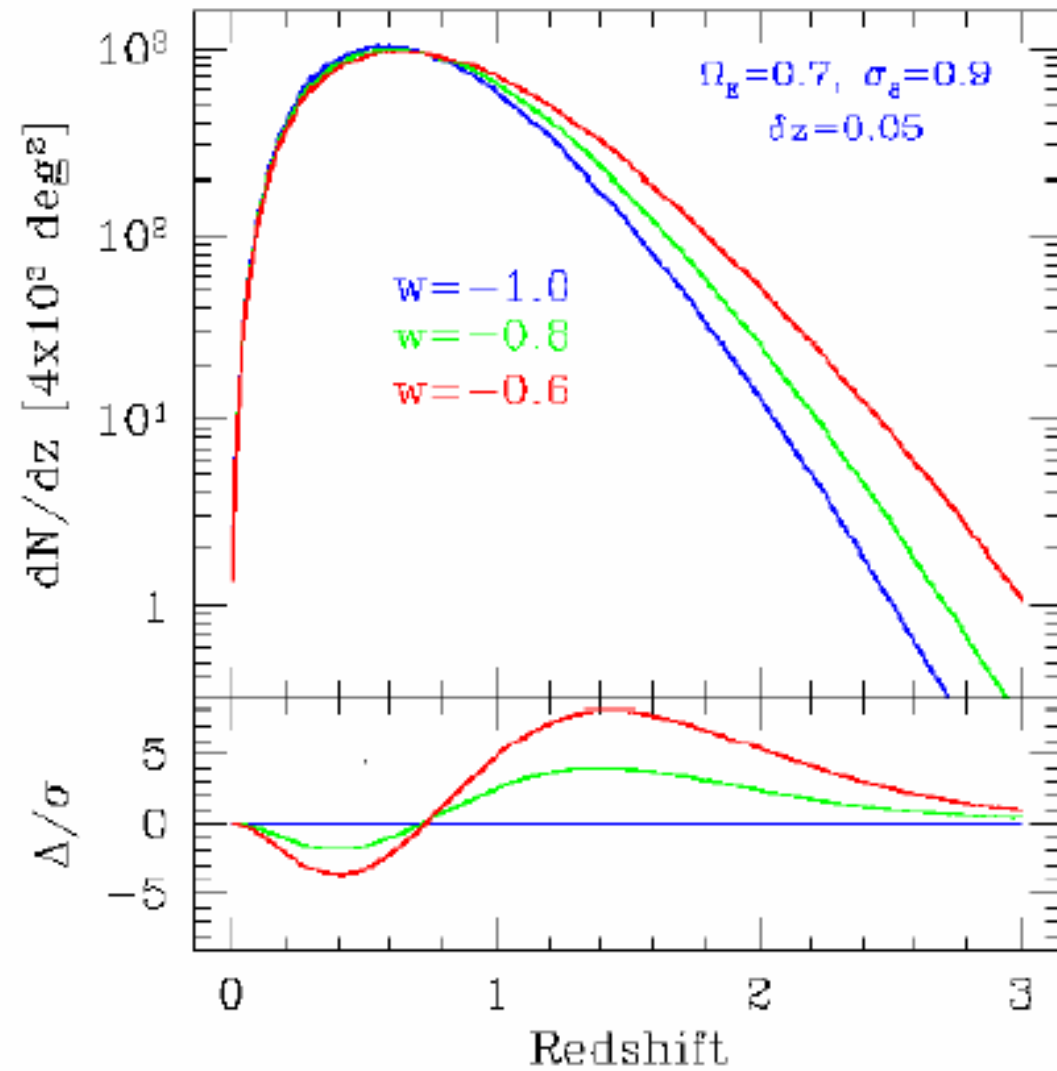
+ 10 graduate students

APEX-SZ

Measure density of galaxy clusters vs. redshift (distance)

Cluster counts together with redshifts determine cluster dN/dz

constrain dark energy equation of state, w

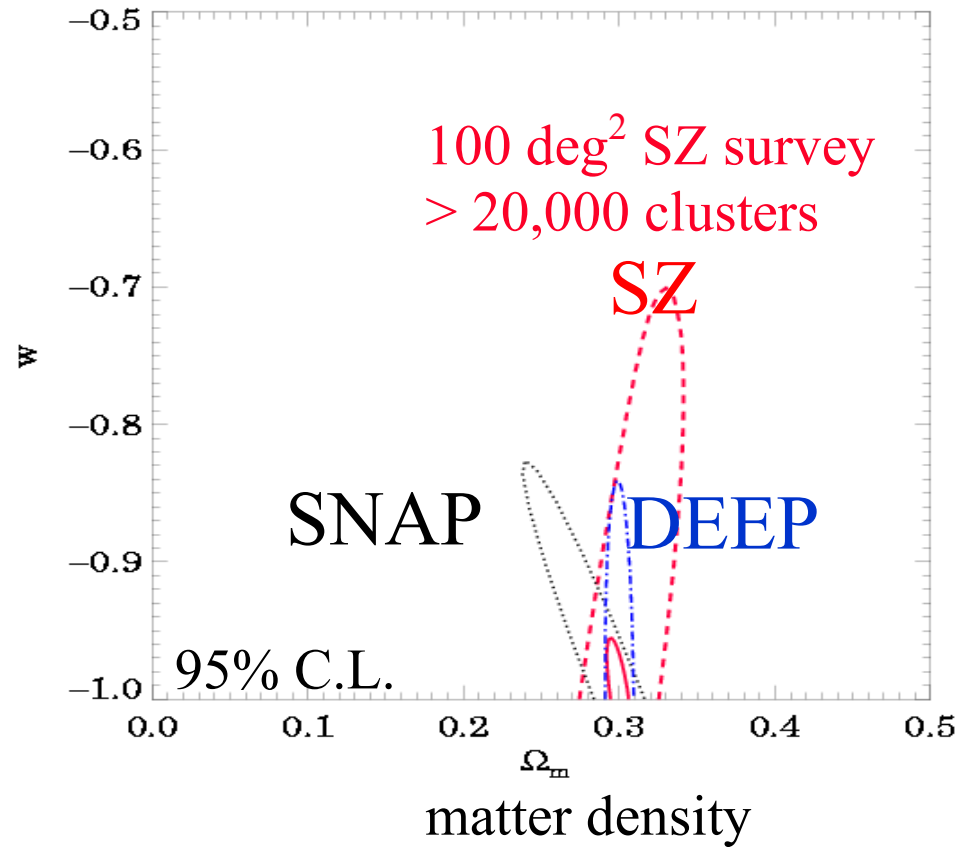


Growth of structure depends on cosmology: Constrain matter density Ω_m

Complementary to DEEP & SNAP

different systematics

different correlations



Measurement Technique: Sunyaev-Zel'dovich Effect

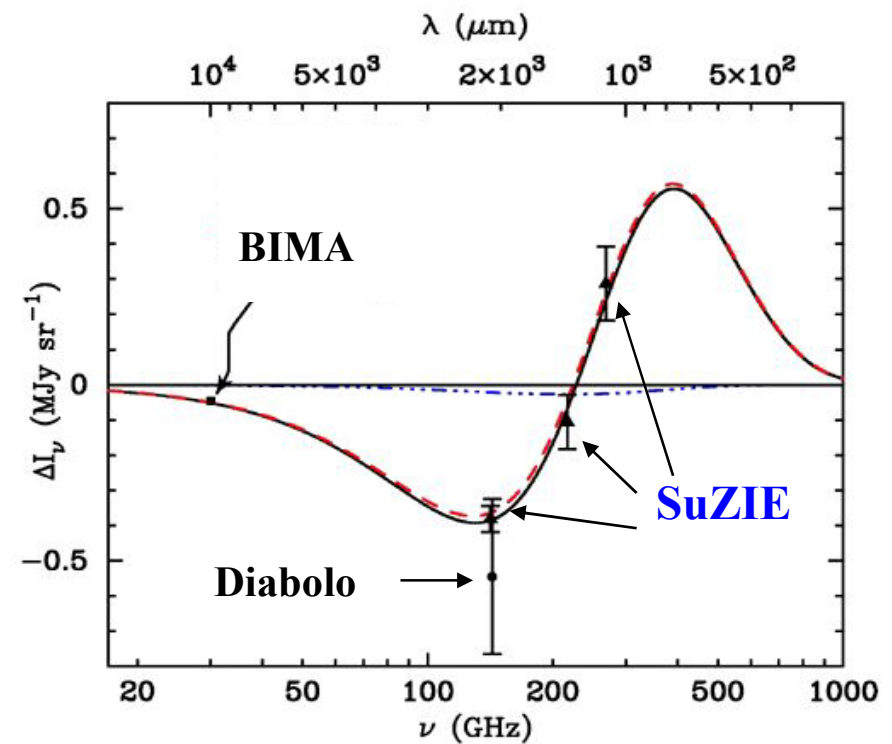
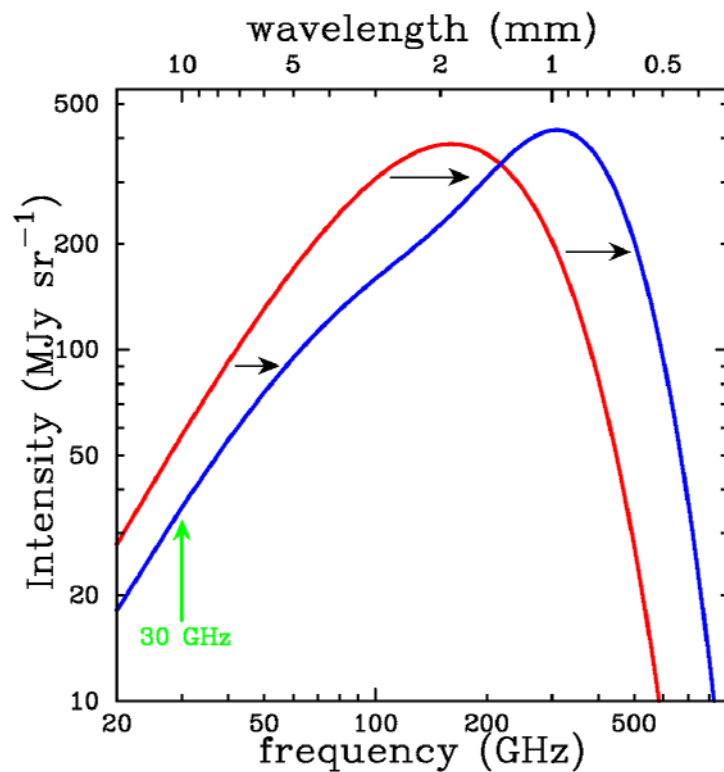
Inverse Compton scattering

Hot gas bound to clusters of galaxies scatters CMB

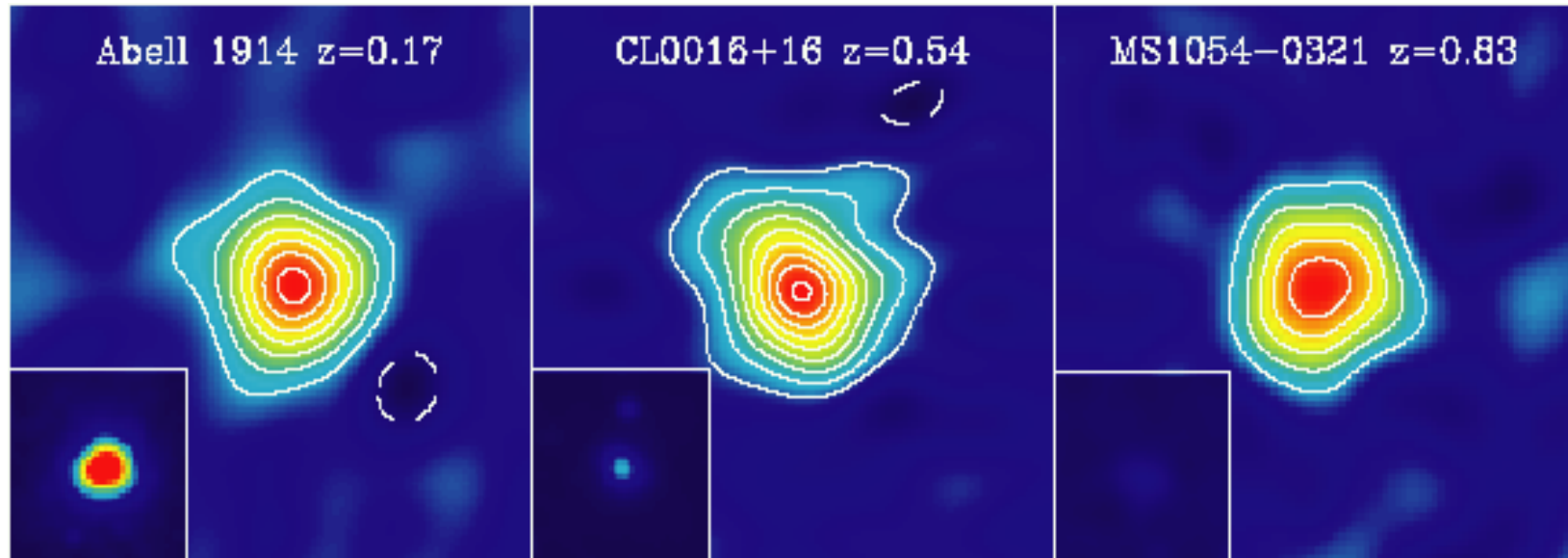
⇒ distorts black-body spectrum

⇒ measure motion of galaxies relative to CMB rest frame

Difference between SZ and black body distributions



SZ effect independent of redshift



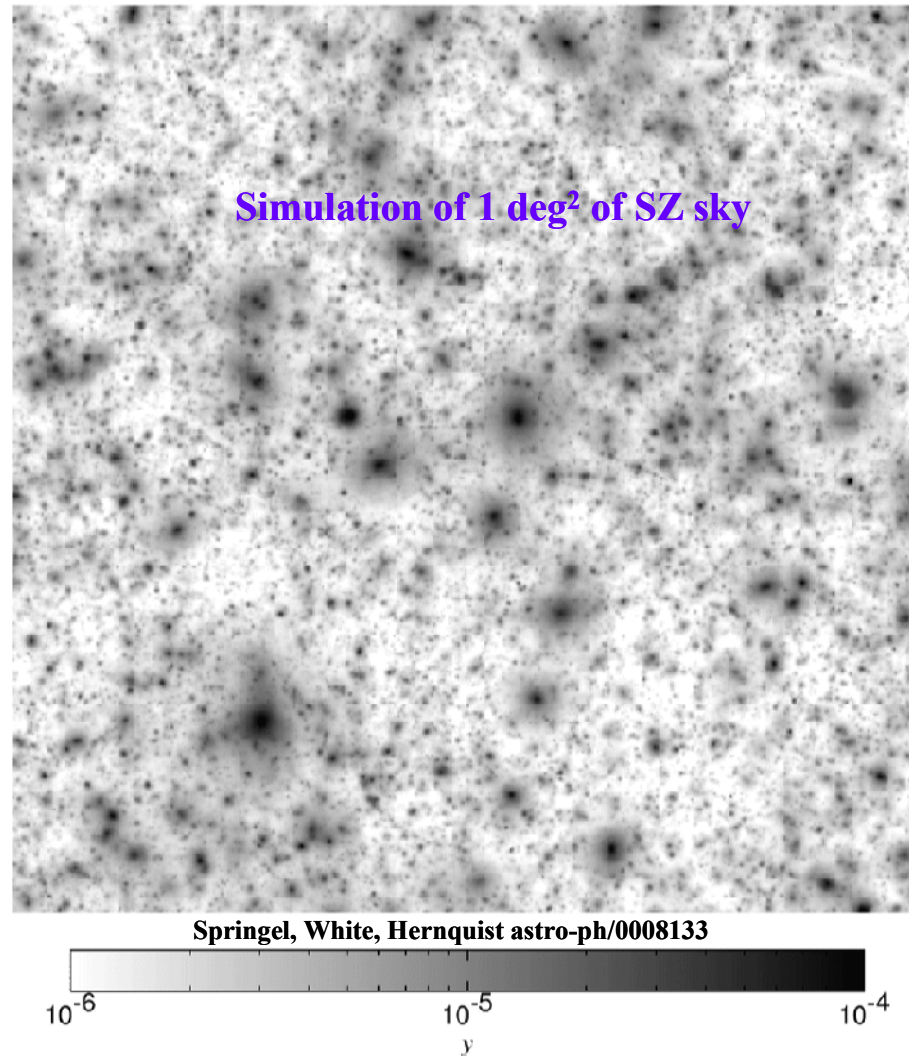
(Holzapfel et al.)

In contrast to x-rays (insets), SZ surface brightness is independent of redshift, so clusters can be seen at any distance.

However, x-ray data needed to determine temperature.

Emerging technique that requires greatly improved arrays.

Galaxy cluster searches



Atacama Pathfinder Experiment (APEX)

Telescope

- Located at 16,500 feet in the Chilean Andes.
- 12m on-axis ALMA prototype
- 45" resolution at 150 GHz
- 30' field-of-view
- Telescope operated by MPIfR/ESO/Onsala.
- Telescope installed in Chile

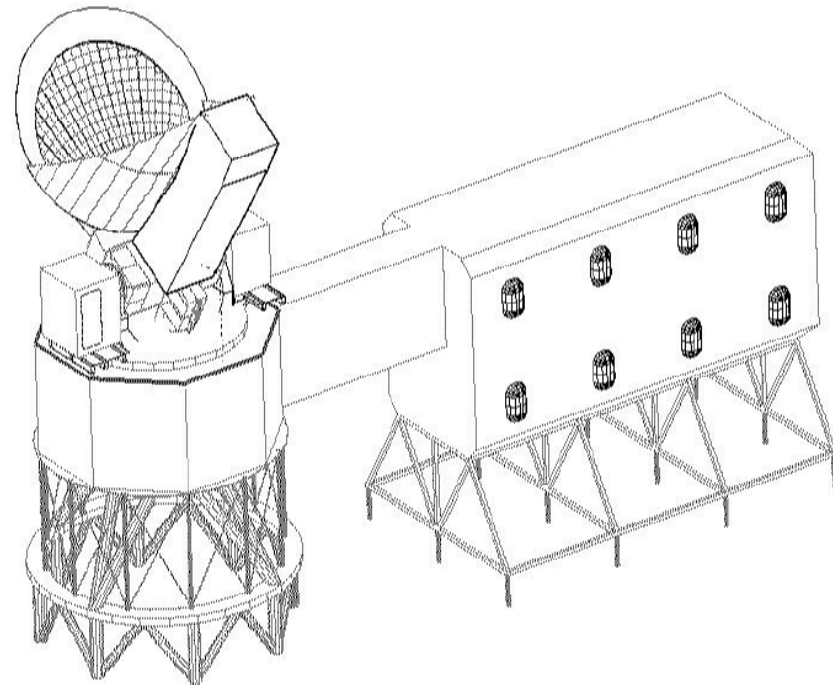
Berkeley SZ receiver

- 300 pixel focal plane array
- funded by NSF astronomy
- 25% of observing time
- First light Fall 2004



South Pole Telescope

- ~1000 pixel focal plane (multiplexed)
- 10m, off-axis design
- 1.3" resolution
- 1 deg. Field of view
- **100% time** SZ observations
- Best mm-wave site
- First light 2006
- Funded by NSF Polar Programs (Chicago, Berkeley, Case Western, SAO)

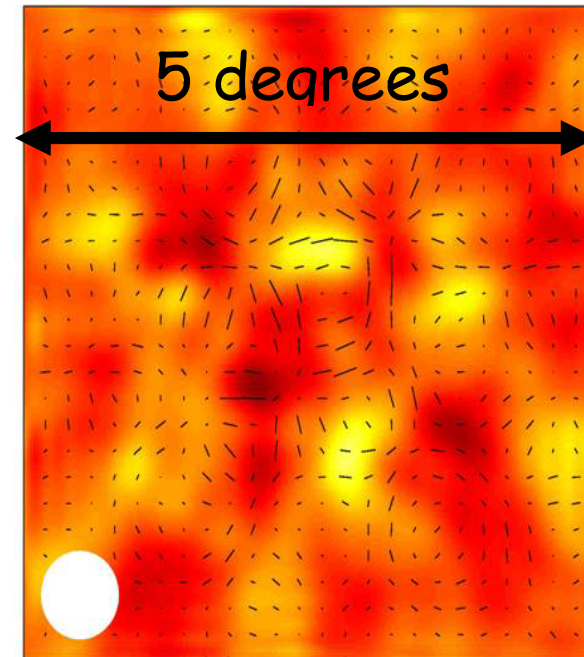


APEX and SPT are complementary:
APEX will be operational 2-3 years before SPT, but SPT will have ~5x faster cluster finding rate.

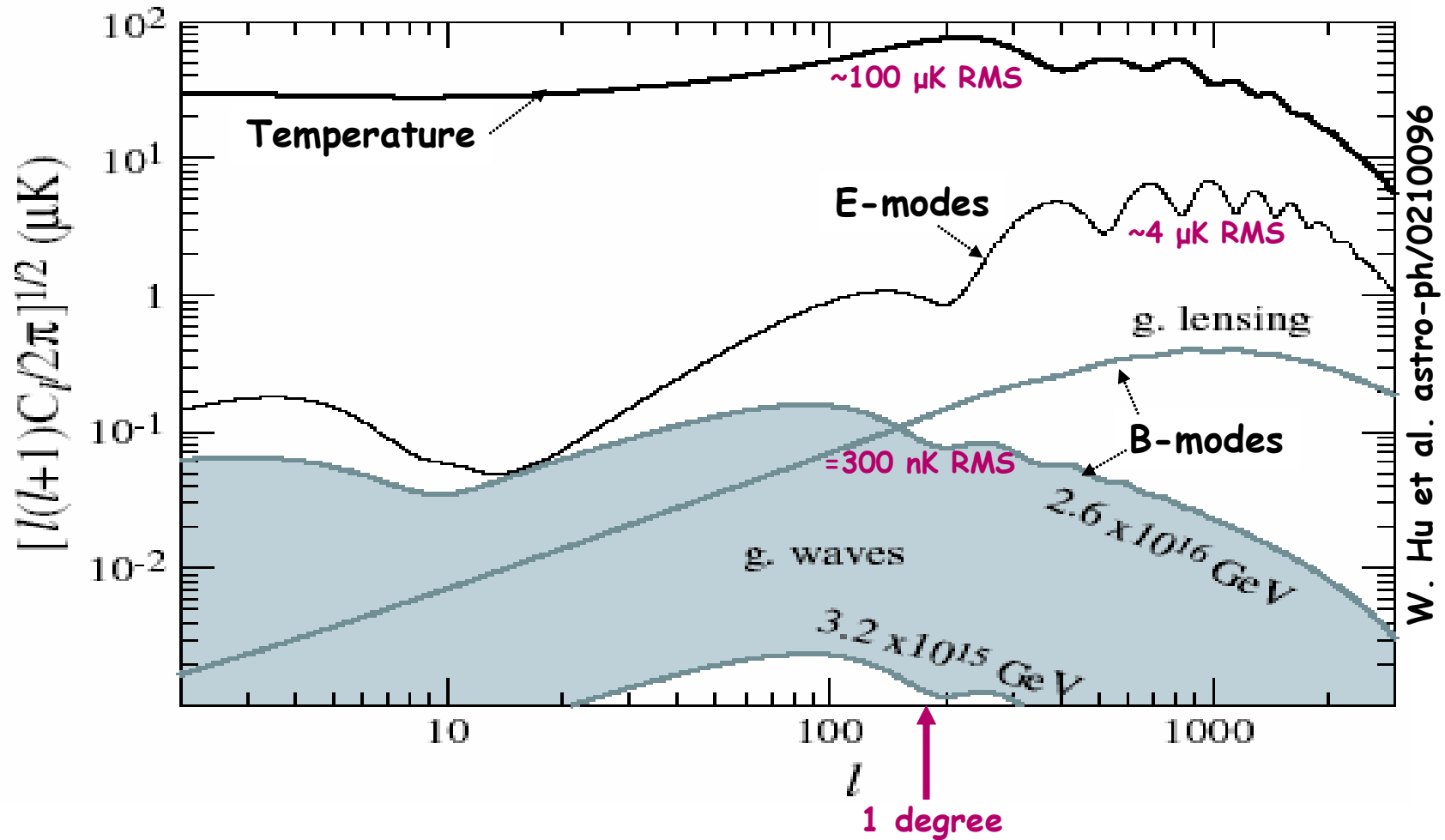
PolarBear

Polarization experiment: detect imprint of gravity waves from Big Bang
("smoking gun" of inflation)

E-mode polarization detected (Carlstrom, et al.):



Gravity waves generate B-modes: Polarization field has net curl.



B-modes are also generated by weak lensing of E-mode polarization
 Gravity wave signature and lensing have different angular scales
 Requires 3m reflector to provide angular resolution.

PolarBear Site: White Mountain, CA (~4000 m)



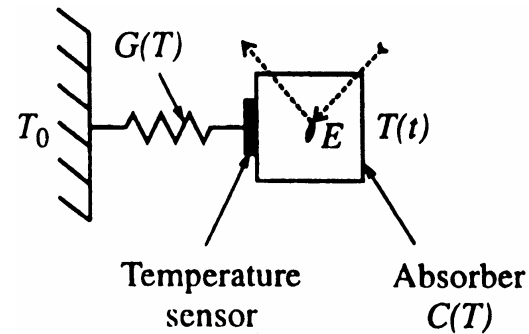
- atmospheric emission is nearly unpolarized.
 - large sky coverage for primordial gravity waves
 - sufficient resolution to measure and subtract out gravitational lensing signal.
 - staged deployment – 300 elements, upgrade to ~3000 pixels
 - multi-frequency polarization sensitive antenna coupled to Transition Edge Sensor bolometers
 - testing facility for future satellite technologies, systematics, and foreground measurements
 - first light 2005(?)
- All of these experiments require major step-up in sensitivity

Measurement Requirements

- 2.7 K black body spectrum: peaks at 150 GHz
- Antenna delivers power proportional to CMB temperature
- 2.7 K signal power: \sim pW
- Next generation experiments aiming for 300 nK resolution
- Bolometers at photon shot noise limit
- 100 - 1000 increase in sensitivity needed
 - increase observing time
 - large bolometer arrays

Thermal Detectors

Basic configuration:



Assume thermal equilibrium:

If all absorbed energy E is converted into phonons, the temperature of the sample will increase by

$$\Delta T = \frac{E}{C}$$

where C the heat capacity of the sample (specific heat x mass).

At room temperature the specific heat of Si is 0.7 J/gK, so

$$E = 1 \text{ keV}, m = 1 \text{ g} \Rightarrow \Delta T = 2 \cdot 10^{-16} \text{ K},$$

which isn't practical.

What can be done?

a) reduce mass

b) lower temperature to reduce heat capacity “freeze out” any electron contribution, so phonon excitation dominates.

Debye model of heat capacity: $C \propto \left(\frac{T}{\Theta}\right)^3$

Example:

$$m = 15 \mu\text{g}$$

$$T = 0.1 \text{ K}$$

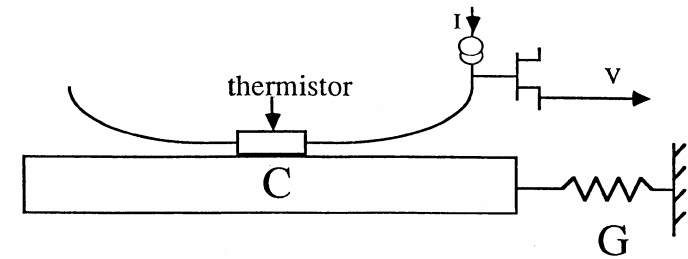
$$\text{Si} \quad \Rightarrow \quad C = 4 \cdot 10^{-15} \text{ J/K}$$

$$E = 1 \text{ keV} \quad \Rightarrow \quad \Delta T = 0.04 \text{ K}$$

How to measure the temperature rise?

Couple thermistor to sample and measure resistance change

Thermistors made of very pure semiconductors (Ge, Si) can exhibit responsivities of order 1 V/K, so a 40 mK change in temperature would yield a signal of 40 mV.



(Sadoulet, et al.)

Superconducting Transition Edge Sensors (TES)

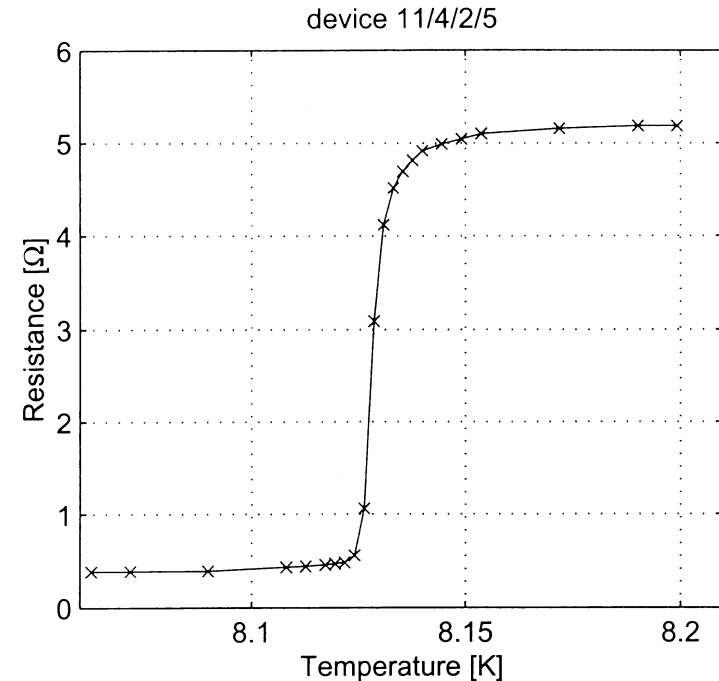
Utilize abrupt change in resistance in transition from superconducting to normal state

The ultimate detection limit is determined by the thermodynamic noise of the sensor and the thermal noise associated with its resistance.

$$P_N = 4kT_S b + \sqrt{4kT_S^2 G b}$$

b = bandwidth

(Jan Gildemeister)



Worldwide activity on cryogenic detectors has led to impressive results, but devices have been

Hand-crafted

Critical to operate

⇒ only small arrays have been used

Recent developments have changed this picture:

1. Voltage-Biased Transition Edge Sensors

⇒ stable and predictable response

2. TES can be monolithically integrated using fabrication techniques developed for Si integrated circuits and micromachining.

⇒ fabricate large arrays with uniform characteristics

Voltage-Biased Transition-Edge Sensors

Required power is of order pW, i.e. voltage of order μV
 current of order μA

Simplest to bias device with a constant current and measure change in voltage

Problem: power dissipated in sensor $P = I^2 R$

Increasing $R \Rightarrow$ Increasing $P \Rightarrow$ Increasing $R \Rightarrow$ Increasing P

\Rightarrow thermal runaway

When biased with a constant voltage $P = \frac{V^2}{R}$

Increasing $R \Rightarrow$ Decreasing $P \Rightarrow$ Decreasing $T \Rightarrow$ Decreasing R

\Rightarrow **negative feedback**

stabilizes operating point

In the transition regime the power is roughly independent of bias voltage.

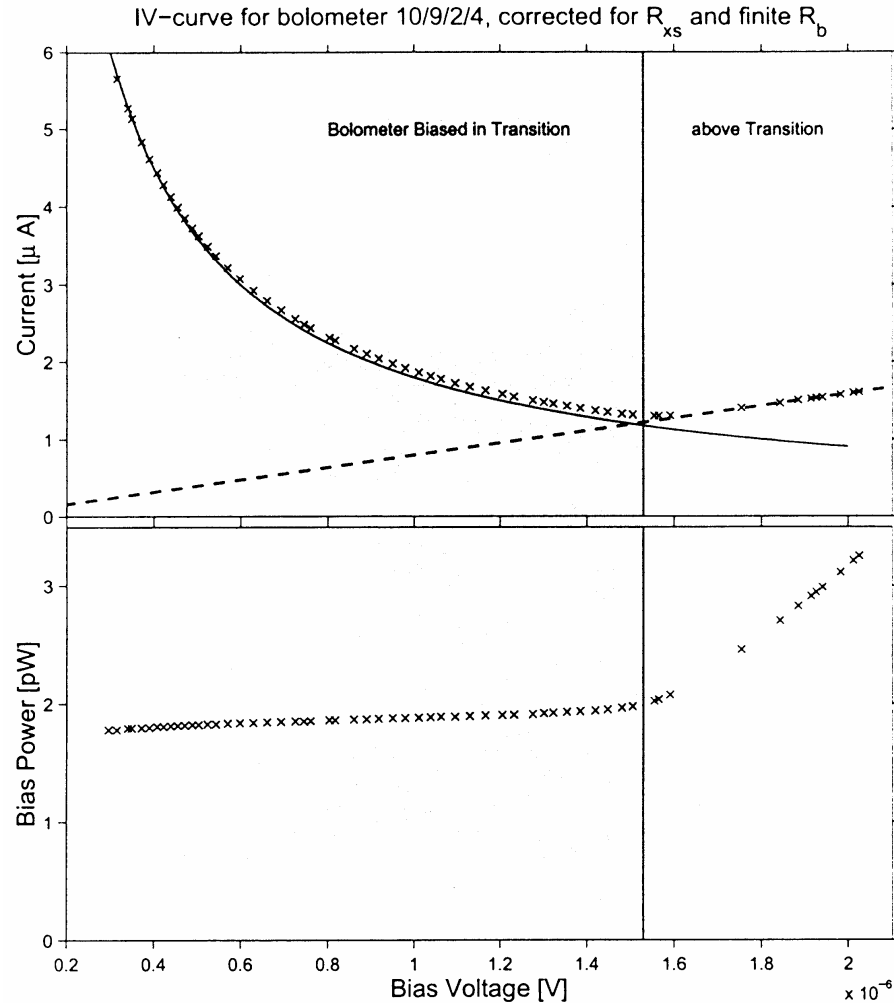
Electrothermal negative feedback keeps total power in bolometer constant.

Change in power due to absorbed radiation must be balanced by change in bias power

$$Q_0 = -V \int_0^{\infty} I(t) dt$$

Signal current proportional to signal power.

⇒ calibration is determined only by magnitude of bias voltage.



from Gildemeister

Important constraint:

Since sensor resistance of order $0.1 - 1 \Omega$, the total external resistance, i.e.

- Internal resistance of voltage source
- Input resistance of current measuring device

must be much smaller to maintain voltage-biased operation, i.e. $< 0.01 - 0.1 \Omega$!

SQUIDs are good match for TES readout

- low temperature device
- very low noise possible
(10 mK noise temperature compared to sensor temperature of 100 – 300 mK)
- low input impedance (input inductance ~ 100 pH)
- adequate gain to drive room-temperature amplifier without significant noise degradation

However,

- Input signal may not exceed 1/4 flux quantum
(output periodic in Φ_0)
- Feedback loop required to lock flux at proper operating point (flux locked loop)

4.SQUIDs

Superconducting Quantum Interference Devices

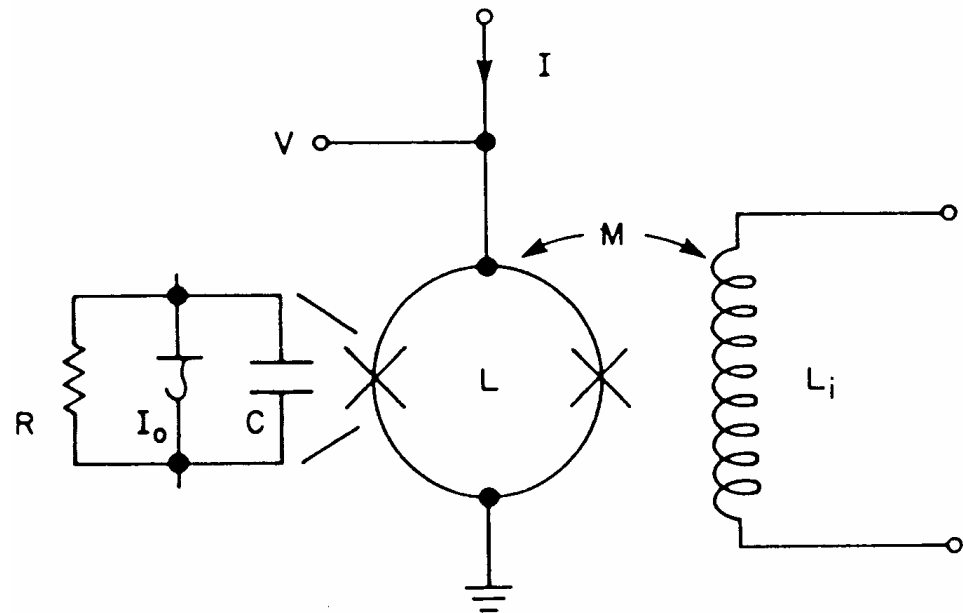
Two Josephson junctions connected in parallel to form superconducting ring:

Two key ingredients:

1. Phase between two tunneling currents in Josephson junction is determined by current.
2. Magnetic flux in superconducting loop is quantized:

$$\Delta\Phi_0 = \frac{\pi\hbar c}{e} = 2.0678 \cdot 10^{-7} \text{ gauss cm}^2$$

$$= 2.0678 \cdot 10^{-15} \text{ Vs}$$



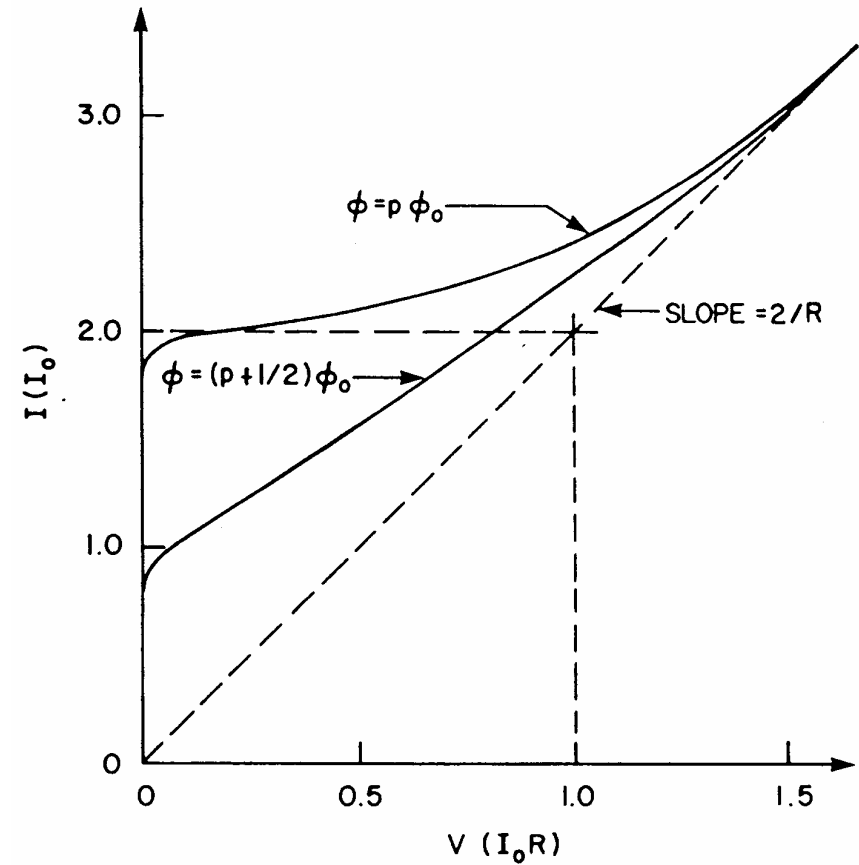
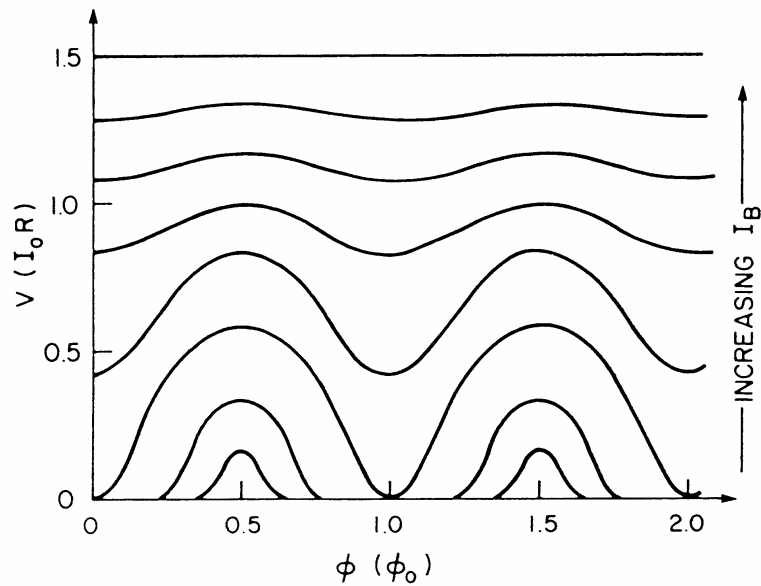
SQUID is biased by current I .

Input signal is magnetic flux due to current through coupling coil L_i .

Output is voltage V .

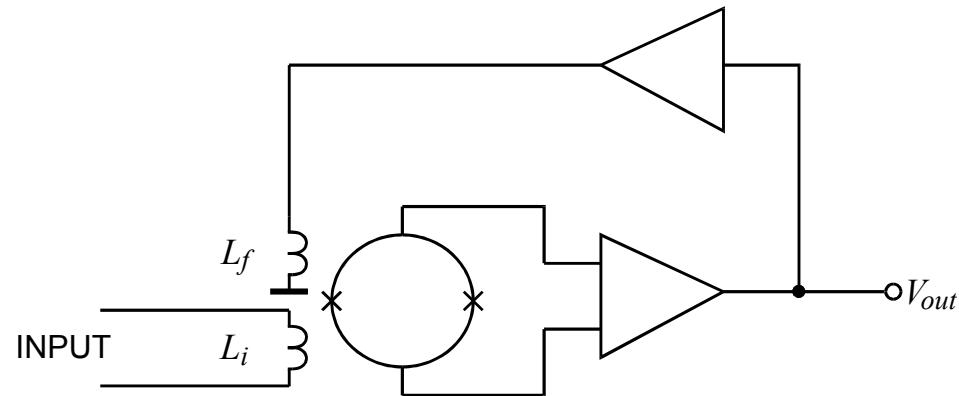
Current-Voltage Characteristics

Output voltage V vs. flux Φ/Φ_0 as bias current I_B is increased



However,

- Input signal may not exceed $\frac{1}{4}$ flux quantum
(output periodic in Φ_0)
- Feedback loop required to lock flux at proper operating point (flux locked loop)



Feedback circuit limits frequency response.

H. Spieler, Frequency Domain Multiplexing for Large-Scale Bolometer Arrays, in Proceedings Far-IR, Sub-mm & mm Detector Technology Workshop, Wolf J., Farhoomand J. and McCreight C.R. (eds.), NASA/CP-211408, 2002 and LBNL-49993

Typical Parameters

| | |
|------------------------|-----------------------------------|
| Operating Temperature: | 0 – 5 K (also high T_C SQUIDs) |
| Flux Sensitivity: | $V_\Phi = 150 \mu\text{V}/\Phi_0$ |
| Flux Noise: | 1 to 10 $\mu\Phi_0$ |
| SQUID Inductance: | 100 – 500 pH |
| Input Inductance: | 10 nH to 1 μH |

Series SQUID Arrays

Array of SQUIDs with
input coils in series and
outputs connected in series.

We use arrays of 100 series-connected SQUIDs (fabricated by NIST).

$$\text{Sensitivity: } \frac{\text{output voltage}}{\text{input current}} = M_i \frac{dV}{d\Phi} \approx 500$$

Monolithic Fabrication of TES Arrays

(Jan Gildemeister et al.)

TES sensor can be fabricated with thin film deposition.

Signal is captured by metallic grid on Si-nitride beams
(7 μm wide x 1 thick)

Sensor in middle of grid:

Ti (500 \AA) – Al(400 \AA) – Ti(500 \AA) – Al(1000 \AA)
(dot in middle of lower figure)

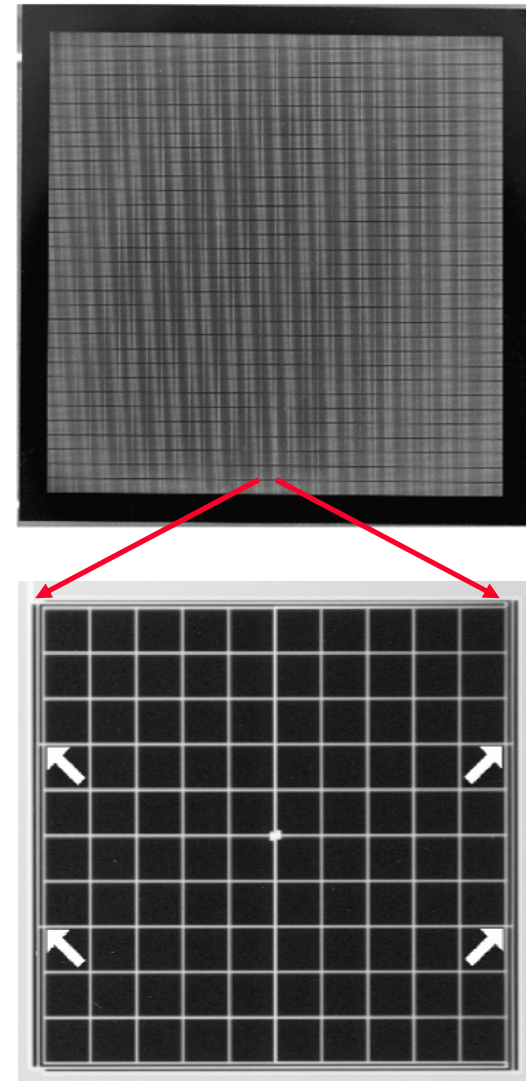
Prototype 32 x 32 Si_2N_3 array:

Grid made from film of low-stress
Si-nitride etched to form beams.

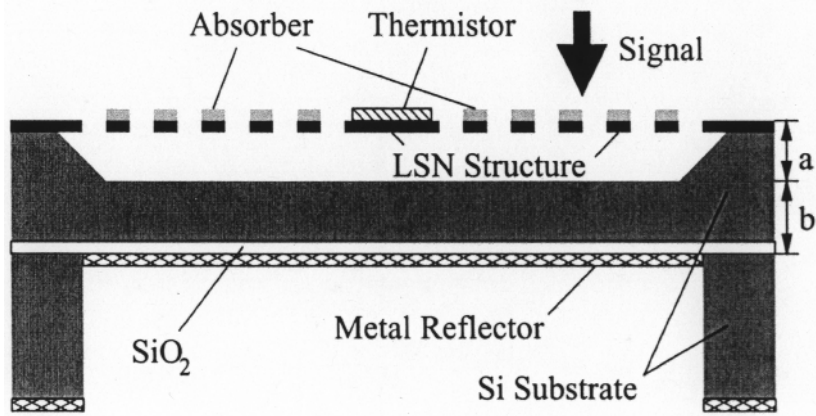
Connected to frame at 4 points
(arrows)

- high thermal resistance
- connections to readout

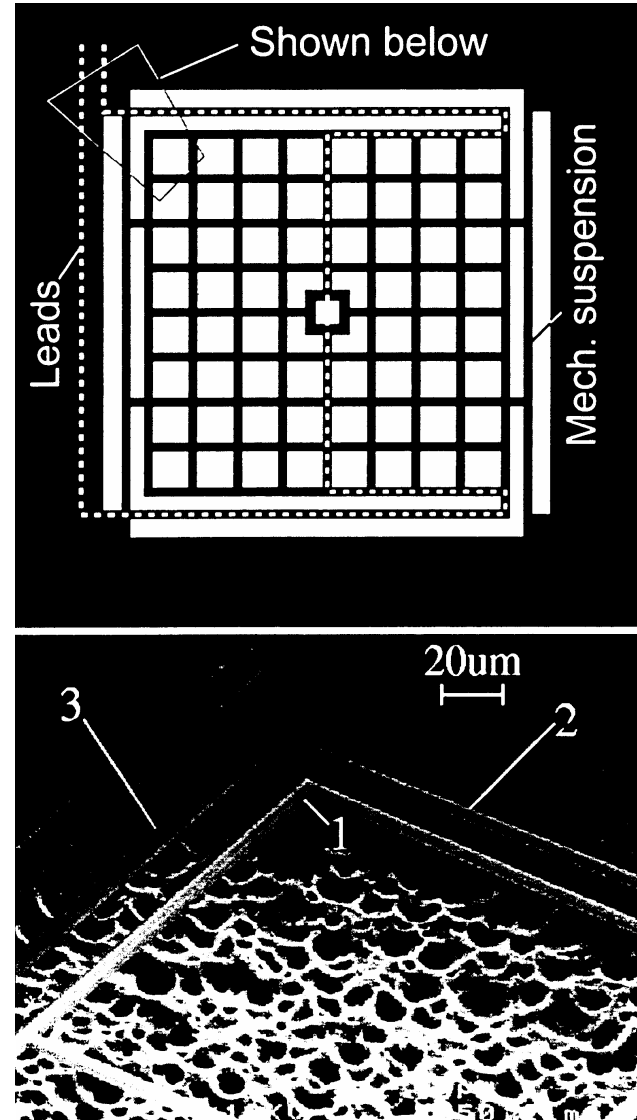
pixel:
1.5 x 1.5 mm^2



Cross Section of Pixel

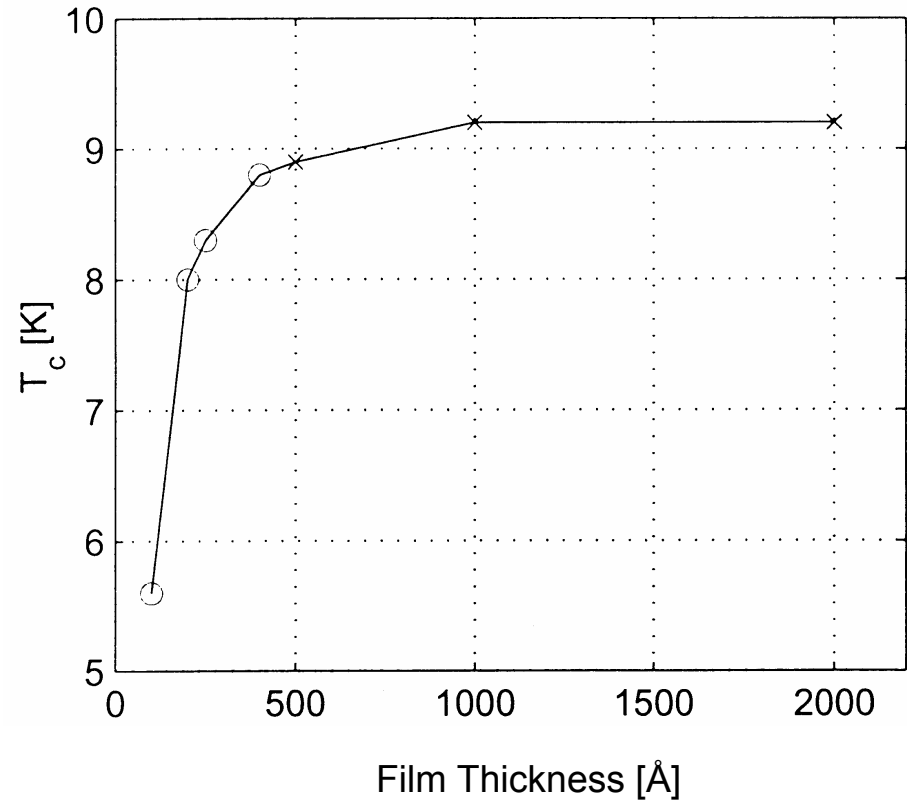


Etch detail



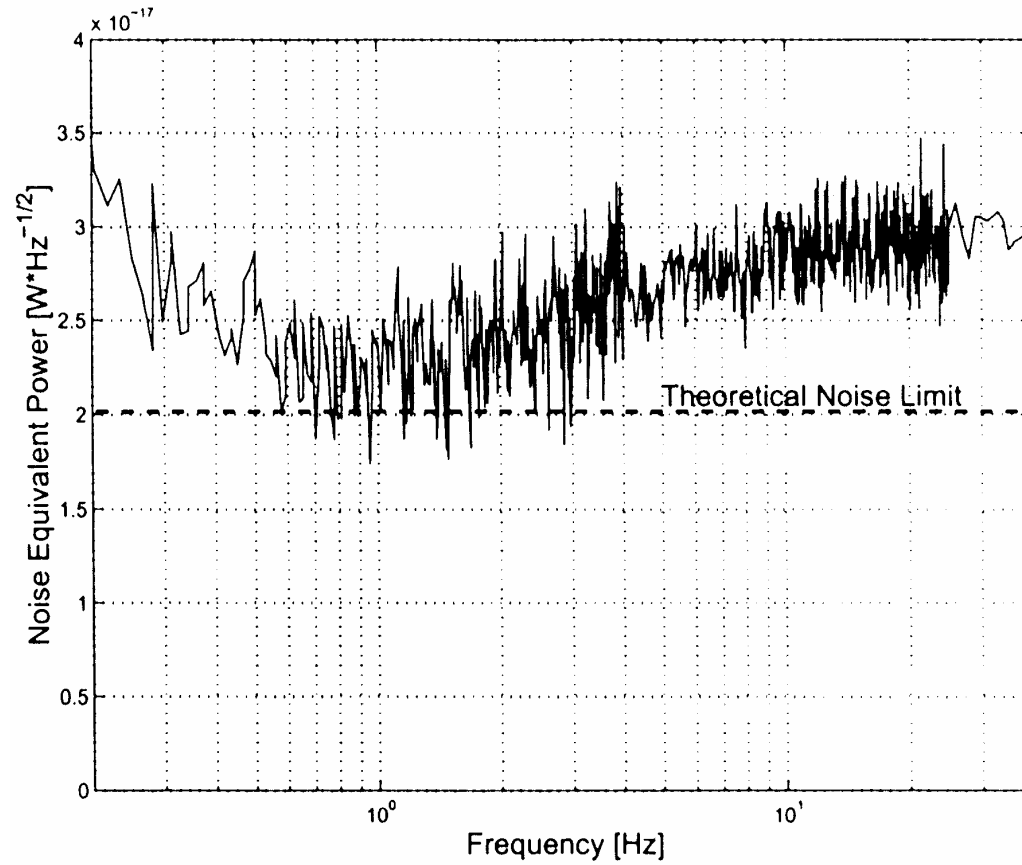
Transition temperature is adjusted by choice of thickness and materials in sensor sandwich:

1. Transition temperature depends on film thickness
2. Thin adjacent layers interact ("Proximity Effect")



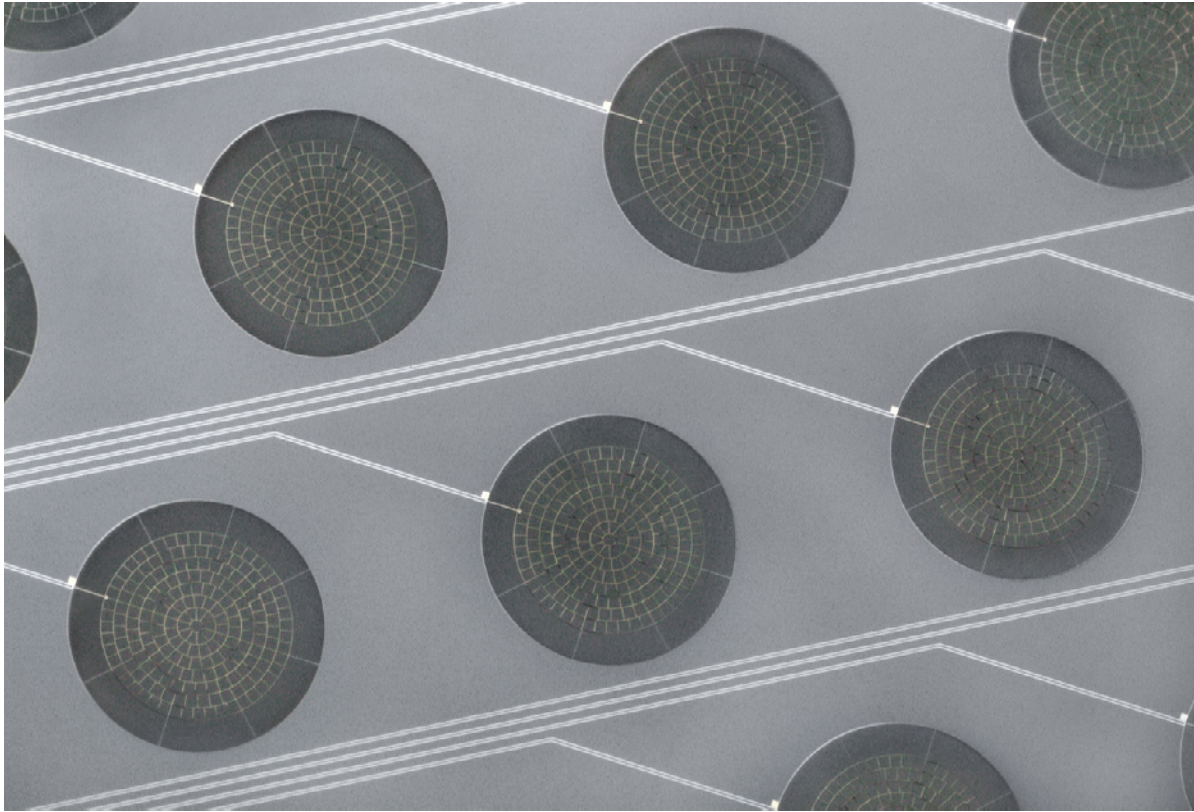
Jan Gildemeister

Measured Noise



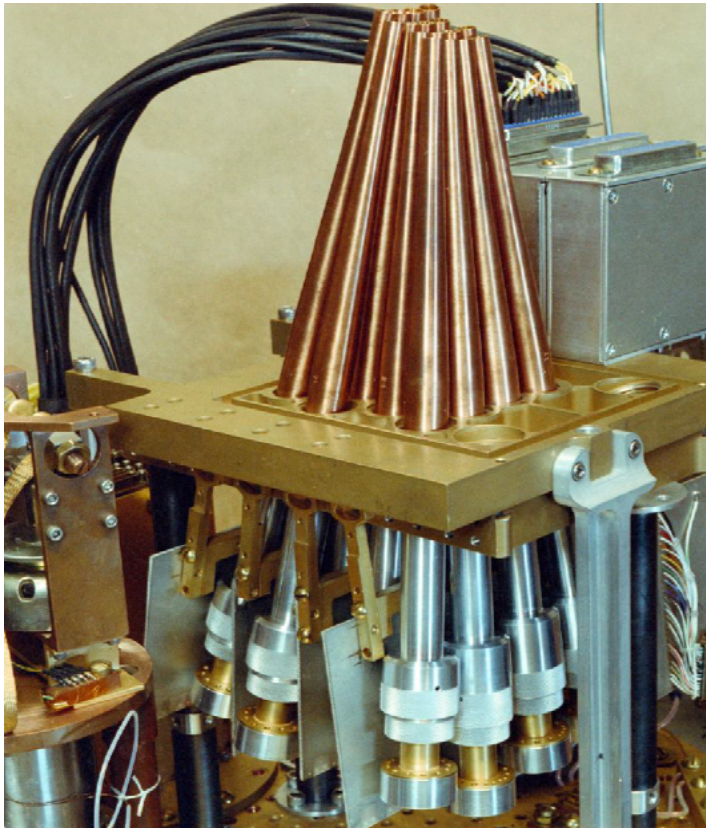
Jan Gildemeister

APEX-SZ Spiderweb Bolometers (Jared Mehl)



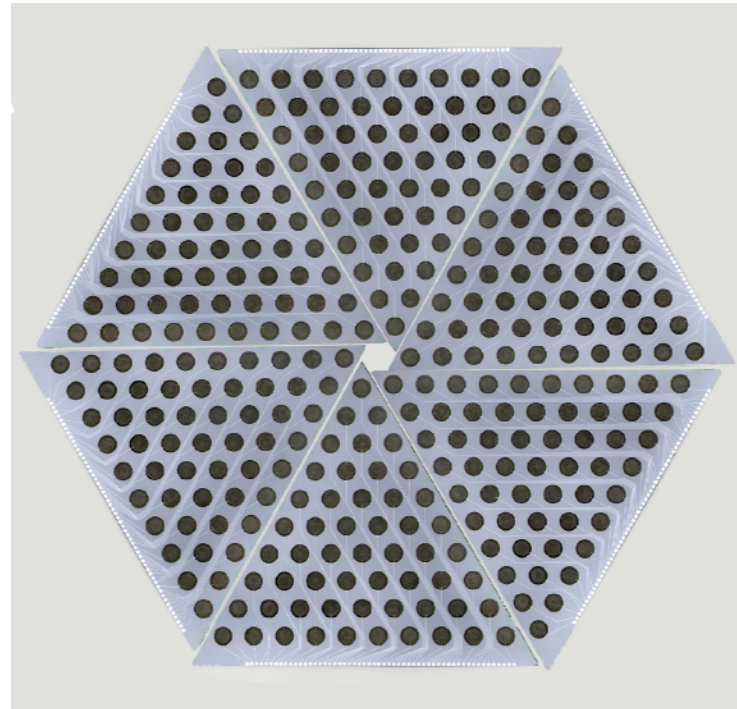
↔
3 mm

OLD



16-sensor MAXIMA Array

NEW



← 15 cm →

300-element APEX-SZ Array

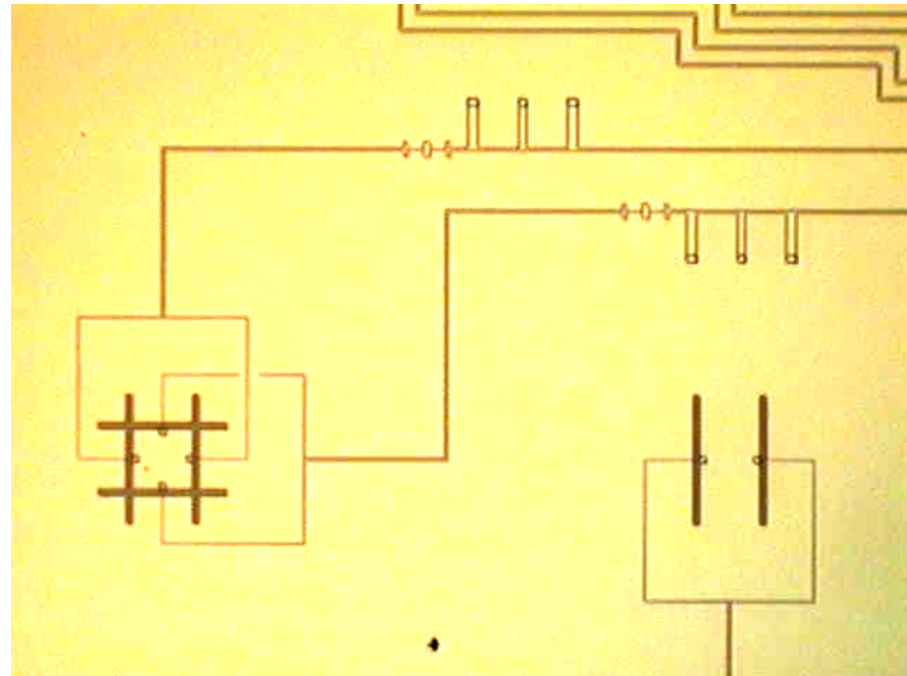
Polarization Receiver

Integrate Antennas + Bandpass Filters + Sensors

(Mike Myers)

Antenna-coupled bolometers

- Monolithically integrate crossed-dipole antennas + bandpass filters with bolometer
- Connect bolometer through transmission line
- Bolometer is load resistor
- Antenna bandwidth allows multiple frequency bands



Sensors at 0.5 K: μW Power Budget

- Arrays with >1000 pixels in development
- Heat leak through wires to 4K stage too large
- Frequency-Domain Multiplexing
 - AC bias each bolometer at different frequency (500 kHz - 1 MHz)
 - signal modulates bolometer current
 - signal in sidebands associated with each carrier frequency
 - each bolometer signal at unique frequency
- ~ 30 bolometers per wire-pair

Modulation Basics

If a sinusoidal current $I_0 \sin \omega t$ is amplitude modulated by a second sine wave $I_m \sin \omega_m t$

$$I(t) = (I_0 + I_m \sin \omega_m t) \sin \omega t$$

$$I(t) = I_0 \sin \omega t + I_m \sin \omega_m t \sin \omega t$$

Using the trigonometric identity $2 \sin \alpha \sin \beta = \cos(\alpha - \beta) - \cos(\alpha + \beta)$ this can be rewritten

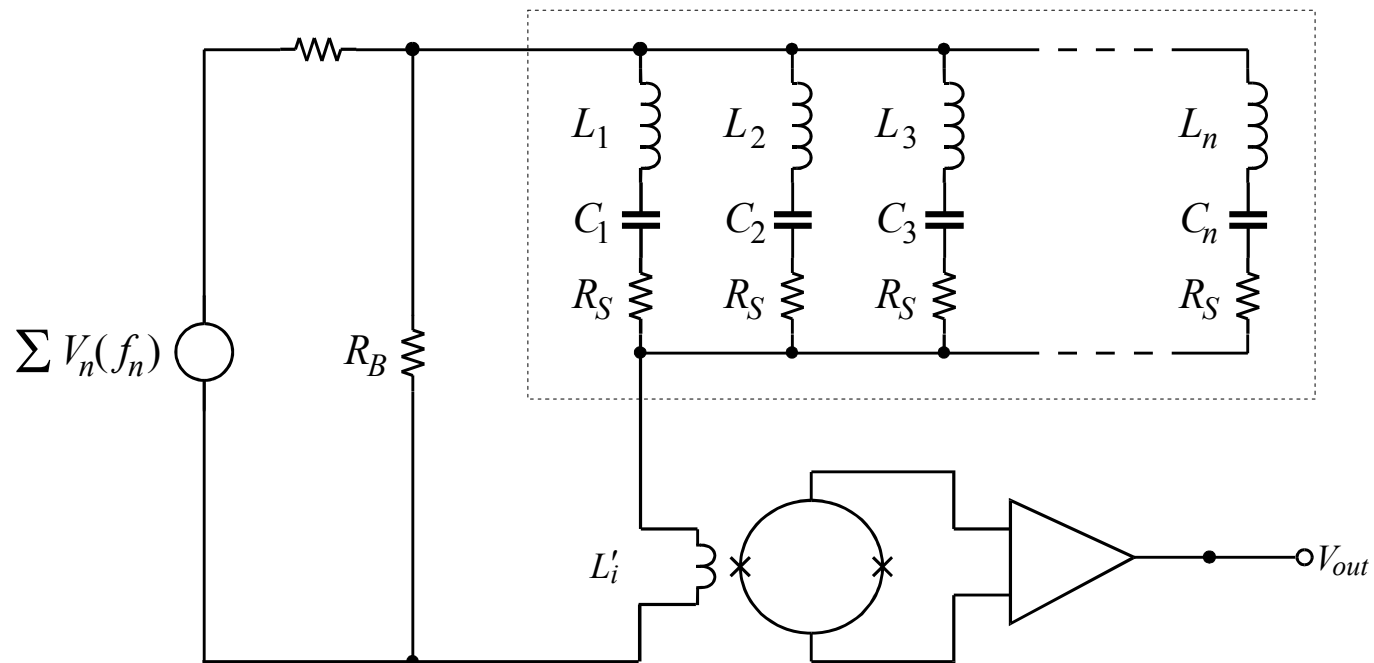
$$I(t) = I_0 \sin \omega t + \frac{I_m}{2} \cos(\omega t - \omega_m t) - \frac{I_m}{2} \cos(\omega t + \omega_m t)$$

The modulation frequency is translated into two sideband frequencies $(\omega t + \omega_m t)$ and $(\omega t - \omega_m t)$ symmetrically positioned above and below the carrier frequency ω .

All of the information contained in the modulation signal appears in the sidebands; the carrier does not carry any information whatsoever.

The power contained in the sidebands is equal to the modulation power, distributed equally between both sidebands.

Frequency-Domain Multiplexer



- All bias frequencies combined on common bias line.
- Tuned circuits route bias frequencies to appropriate bolometer
- Individual currents summed at low-impedance SQUID amplifier

1. The sensors are AC biased by the frequency generator at the left of the figure. The AC drive signal is applied as a comb spectrum $V(t) = \sum V(f_n) = \sum V_n \cos(\omega_n t)$. The bias resistance R_B is much smaller than the sensor resistance R_S to ensure voltage-biased operation.
2. The individual series resonant circuits $L_n C_n$ are set to the component frequencies of the drive spectrum, so that each leg of the sensor array is driven predominantly by only one frequency f_n .
3. Signal power absorbed by the sensor modulates the current flow through the tuned circuit, translating a signal spectrum Δf_s into sidebands $f_n \pm \Delta f_s$ above and below the corresponding carrier frequency.
4. The sum of all sensor currents is sensed by an output current amplifier.

Its input impedance must be much smaller than the sensor resistance over the whole range of bias frequencies, again to ensure voltage-biased operation.

5. A bank of frequency-selective demodulators extracts the individual signals from the composite signal.

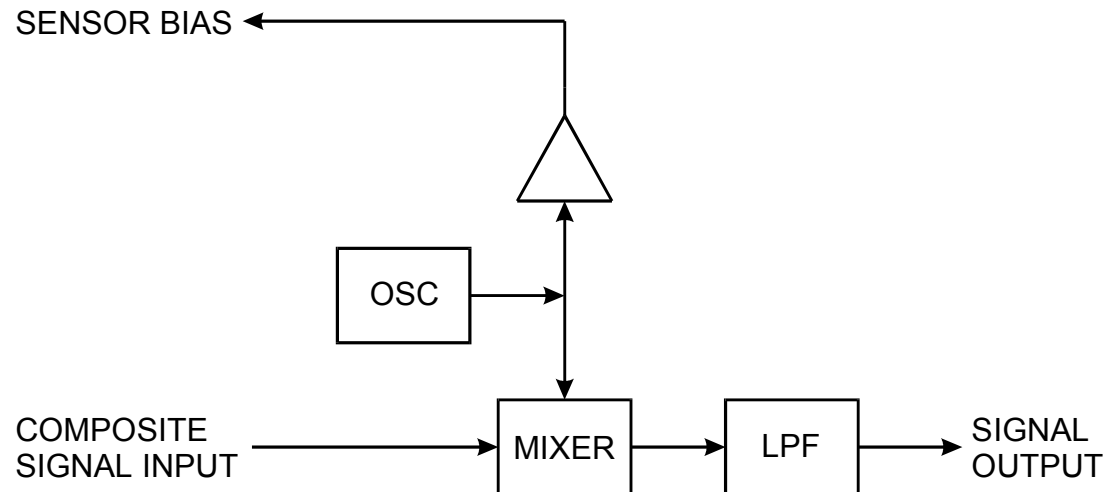
Demodulation

The same carrier signal that biases the sensor is used to translate the sideband information to baseband.

The mixer acts analogously to a modulator, where the input signal modulates the carrier, forming both sum and difference frequencies.

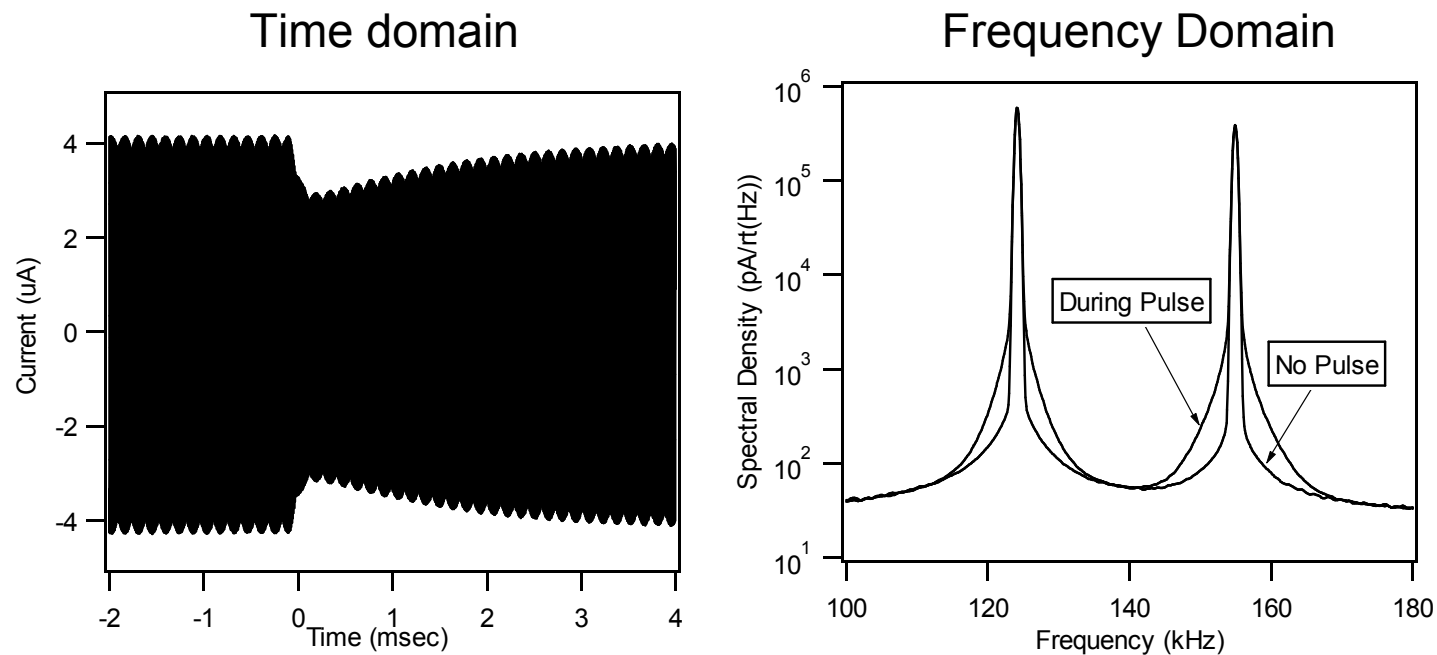
In the difference spectrum the sidebands at $f_n \pm \Delta f_S$ are translated to a frequency band $f_n - (f_n \pm \Delta f_S) = 0 \pm \Delta f_S$.

A post-detection low-pass filter attenuates all higher frequencies and determines the ultimate signal and noise bandwidth.



Frequency-Domain MUX Demonstrated with X-Ray Micro-Calorimeters

LLNL/UCB/LBNL collaboration



Energy resolution of 60 eV FWHM unaffected by multiplexer.
 MUXing \Rightarrow increase active area, overall rate capability

Summary: Breakthrough in Cryogenic Detectors

- Sensitivity approaching quantum level at mm wavelengths
- Voltage-biased superconducting transition edge sensors
 - ⇒ stable operation
predictable response
- Sensors can be fabricated using monolithic technology developed for Si integrated circuits, micro-mechanics
 - ⇒ economical fabrication of large sensor arrays
- Challenge: Readout
(multiplexing of many channels)
prototypes tested, but much work to do
- great opportunities for students + post-docs!

Exciting Times in Physics!

- Dark Matter and Dark Energy comprise 95% of the universe.
- We don't know what the dark matter is, nor do we have any credible explanation of dark energy.
- All of the physics and chemistry of the past ~400 years has been directed at understanding only 5% of the universe!
- We may find the “new physics” by looking 12.7 billion years into the past.
- One thing is clear - new imaging detectors will play a key role in solving these mysteries.

